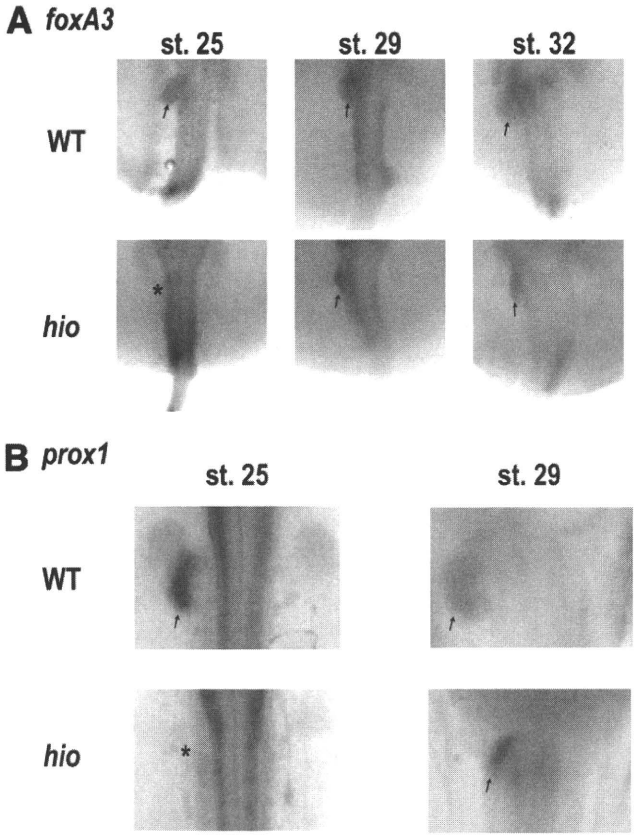

Fig. 3. Impaired hepatic bud formation but normal pancreas in *hio* embryos. (A) Whole-mount *in situ* hybridization to detect *foxA3* expression in WT and *hio* mutant embryos at stages 25, 29, and 32. Arrows indicate hepatic buds derived from the foregut. Asterisk indicates that no hepatic bud is present in the *hio* mutant at stage 25. (B) Whole-mount *in situ* hybridization to detect *prox1* expression in WT and *hio* mutant embryos at stages 25 and 29. Arrows indicate hepatic region. Asterisk indicates that no *prox*1 expression is observed in the *hio* mutant at stage 25. For A and B, images shown are single examples representative of more than 20 embryos examined per group.

cell differentiation or liver functions at later stages of embryogenesis.

Stafford and Prince[22] have reported that hepatic and pancreatic cell markers are undetectable in zebrafish *nls* embryos. To investigate whether the *hio* mutation affected pancreas development in medaka, we carried out *in situ* hybridization using probes for the *pdx1* and *insulin* genes. We observed *pdx1*-expressing cells in the pancreatic primordium region in both WT and *hio* embryos at stage 28 (Fig. 4C). Furthermore, *insulin*-expressing cells were present in both WT and *hio* embryos at stage 30 (Fig. 4D). Thus, unlike its effects on liver development, the medaka *hio* mutation does not appear to affect pancreas development. This result stands in contrast to the zebrafish *nls* mutation, which severely impairs the development of both the liver and the pancreas.

wnt2bb *Expression in the LPM Is Lost in* hio *Embryos.* It has been shown in zebrafish that mesodermal *wnt2bb* expression promotes liver specification.[17] It is also known that the *wnt2ba* gene acts downstream of RA signaling and regulates pectoral fin development in zebrafish.[7,20] The *wnt2ba* and *wnt2bb* genes are both members of *wnt2b* gene family that exists in both zebrafish and medaka. These observations suggested to us that Wnt2bb might be a good candidate for the key molecule regulating piscine liver specification downstream of RA signaling. To explore this hypothesis, we examined *wnt2bb* expression in *hio* embryos. At stage 22, no *wnt2bb* expression in the LPM was observed in either WT or *hio* embryos (Supporting Fig. 4). However, by stage 24, *wnt2bb* expression in the LPM directly adjacent to the liver-forming endoderm was induced in WT embryos but not in *hio* embryos (Fig. 5A, left panel). These results suggest that the *hio* mutation causes a loss of *wnt2bb* gene

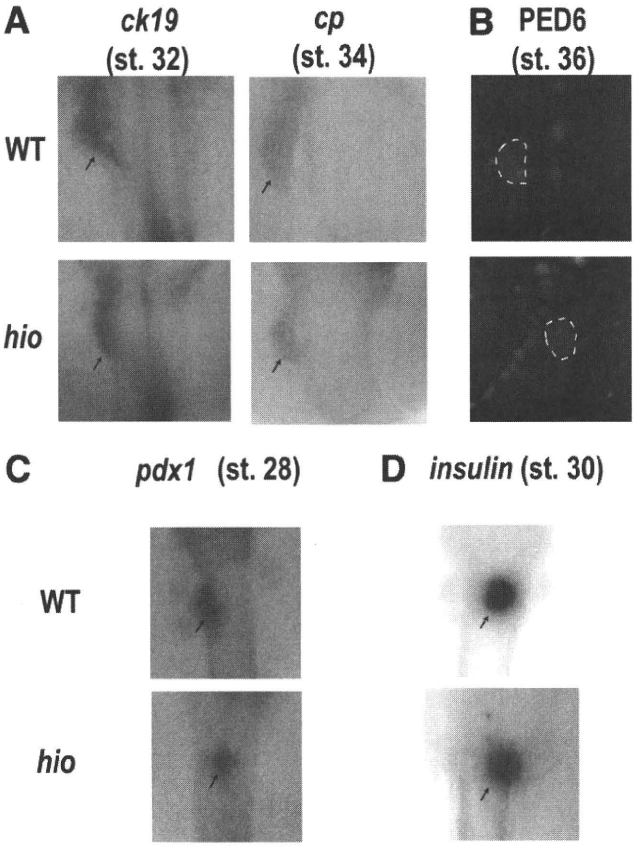

Fig. 4. Normal hepatic cell differentiation and function and pancreatic development in *hio* embryos. (A) Whole-mount *in situ* hybridization of WT and *hio* mutant embryos to detect *ck19* expression by cholangiocytes at stage 32, and *cp* expression by hepatocytes at stage 34. Arrows indicate *ck19*-positive or *cp*-positive livers. (B) WT and *hio* mutant embryos at stage 36 were treated with PED6 to assay liver lipid metabolism. White dashed lines indicate green fluorescence attributable to PED6 metabolites. (C) Whole-mount *in situ* hybridization to detect *pdx1* expression (arrows) in WT and *hio* mutant embryos at stage 28. (D) Whole-mount *in situ* hybridization to detect *insulin* expression (arrows) in WT and *hio* mutant embryos at stage 30. For A-D, images shown are single examples representative of more than 10 embryos examined per group.

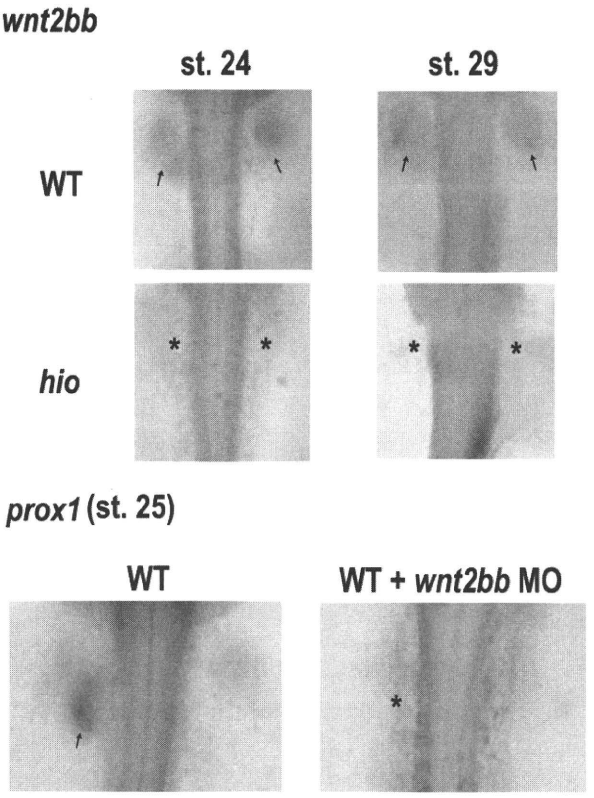

Fig. 5. Impaired *wnt2bb* expression in *hio* embryos. (A) Whole-mount *in situ* hybridization to detect *wnt2bb* expression in WT and *hio* mutant embryos at stages 24 and 29. Arrows indicate *wnt2bb* expression in the WT. Asterisks indicate the lack of *wnt2bb* expression in *hio* mutant embryos. (B) Whole-mount *in situ* hybridization to detect *prox1* expression in WT and *wnt2bb*-morphant (MO) embryos at stage 25. Arrow indicates *prox1* expression in the WT hepatic region. Asterisk indicates the lack of *prox1* expression in the MO embryo. Images shown are single examples representative of more than 20 embryos examined per group.

expression. Interestingly, *wnt2bb* still had not been expressed in the *hio* LPM at stage 29, when the liver bud forms (Fig. 5A, right panel). Thus, the small livers that eventually appear in medaka *hio* mutants seem to form independently of Wnt2bb signaling, just as occurs in zebrafish *prt* mutants.

To investigate whether *wnt2bb* positively regulates liver specification in medaka as it does in zebrafish, we injected *wnt2bb*-specific morpholino antisense oligonucleotides (*wnt2bb*-MO) into the cytoplasm of one-cell stage WT embryos and evaluated the outcome by *in situ* hybridization using a *prox1* probe. We found that, like *hio* embryos, WT medaka embryos that had been injected with *wnt2bb*-MO lacked *prox1* expression (Fig. 5B). These results suggest that Wnt2bb signaling is responsible for liver specification in medaka.

In conclusion, our study has shown that the *hio* mutation in medaka impairs liver specification by abrogating *wnt2bb* expression. Our data are thus the first genetic evidence that RA signaling positively regulates liver specification by inducing *wnt2bb* expression.

Discussion

Function of RA Signaling in Pectoral Fin and Liver Development in Medaka. In this study, we examined the role of RA signaling during embryogenesis by characterizing medaka *hio* mutants. These mutants bear an alteration to the *raldh2* gene (Fig. 1) that encodes the enzyme principally responsible for RA synthesis, and we interpret that this is a nearly null mutation because the phenotypes of *hio* mutant are similar to that of RALDH2 morphants (Fig. 2 and Supporting Fig. 1). The *hio* mutants exhibit two prominent phenotypes: missing pectoral fins and a small liver (Fig. 2 and Supporting Fig. 1). Work in mouse, chick, and zebrafish has shown that RA signaling from the somitic mesoderm is essential for limb induction and is mediated by the expression of downstream factors such as *wnt2ba* and *tbx5*.[7-14] We show that the *hio* mutation in medaka leads to defects in pectoral fin development and *tbx5* and *wnt2ba* expression (Supporting Fig. 2). Thus, our results indicate that RA signaling is crucial for fin specification in medaka and show that limb induction signaling is conserved across a broad range of species (Fig. 6, right part). Significantly, our work has also uncovered a role for RA signaling in liver development. We have demonstrated that the *hio* mutation retards the formation of hepatic buds from the foregut (Fig. 3A) and causes a profound defect in liver specification (Fig. 3B). In addition, we have shown that the *wnt2bb* expression required for the regulation of liver specification is undetectable in the LPM of *hio* embryos (Fig. 5A). Our data constitute the first genetic evidence that RA signaling regulates vertebrate liver specification by inducing *wnt2bb* gene expression (Fig. 6, left part). Previously, Wang et al.[23] reported that liver growth is severely affected in RALDH2-deficient mouse embryos. Thus, RA signaling in liver specification may be conserved among other species.

Molecular Mechanisms Regulating the Development of Pectoral Fins and Liver. There are several similarities in the signaling pathways governing pectoral fin and liver organogenesis. During zebrafish pectoral fin development, RA signaling induces *wnt2ba* expression, which in turn induces *tbx5* expression. *Tbx5* is a key molecule that regulates the expression of downstream effectors such as the *fgf* and *bmp* family members *fgf24*, *fgf10*, and *bmp2b*.[7,16] Thus, limb induction requires a sequential RA → Wnt → Tbx → Fgf + Bmp signaling cascade. A parallel situation may exist for liver specification in medaka. Wnt2bb, Tbx3, Fgf, and Bmp have all been shown to positively regulate the development of this organ in mice or zebrafish.[17,18,24] In this study, we showed

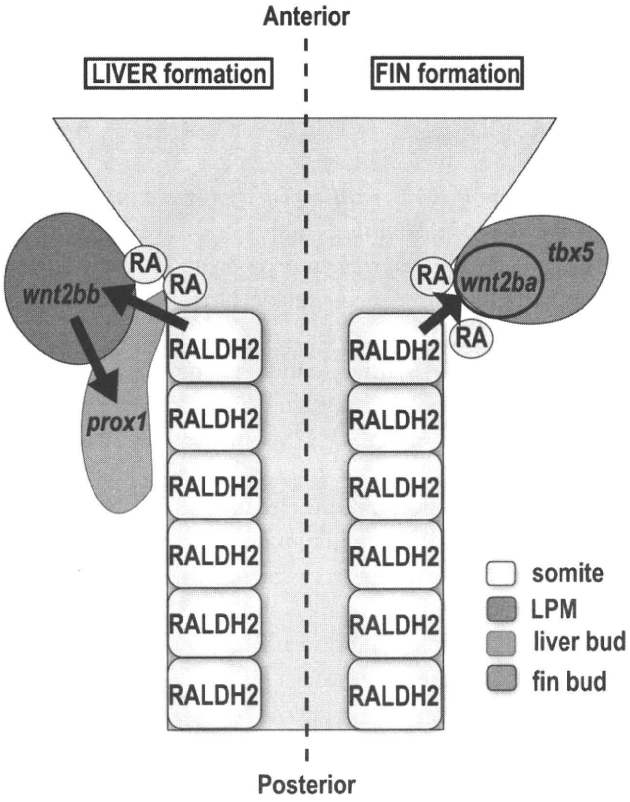

Fig. 6. Schematic model of RA signaling during liver and pectoral fin formation in a WT medaka embryo. (Left) During liver formation in medaka, RALDH2 expression in the somites results in the production of RA that induces *wnt2bb* expression. This Wnt2bb then induces *prox1* expression in the liver bud, which in turn drives hepatocyte migration.[30] (Right) During fin formation, RALDH2 expression in the somites results in the production of RA that induces *wnt2ba* and *tbx5* expression in the fin bud that drives fin cell differentiation.

that RALDH2 drives *wnt2bb* expression during liver specification in medaka (Fig. 5). Based on the proposal of Shin et al.[18] that Fgf and Bmp act downstream of Wnt2bb during liver specification, the sum total of all these results suggests that liver specification also requires a sequential RA → Wnt → Fgf + Bmp signaling cascade. Intriguingly, we found that RA signaling induced *tbx3* expression in medaka (Supporting Fig. 5). However, our morpholino studies showed that RA signaling associated with liver formation can regulate *tbx3* expression without involving Wnt2bb (Supporting Fig. 5). These data indicate that Tbx3 can act downstream of RA signaling, but it is likely that other T-box family members are involved in the putative RA → Wnt → Tbx → Fgf + Bmp signaling cascade that drives liver development. We are continuing our search for the identity of this transcription factor.

Differential Requirements for Liver and Pectoral Fin Specification During Embryogenesis. A sequential RA → Wnt → Tbx → Fgf + Bmp signaling cascade is indispensable for the limb induction process that underlies pectoral fin development. Alterations in *raldh2* such as the medaka *hio* and zebrafish *nls* and *nof* mutations lead to an absence of pectoral fins, as does knockdown of *wnt2ba* using MO in WT zebrafish.[8,10,16] Notably, these mutants and morphants never form pectoral fins during the entire course of embryogenesis. Conversely, a sequential RA → Wnt → Fgf + Bmp signaling cascade is not indispensable for liver specification, because medaka *hio* mutants and zebrafish *prt* mutants are able to form a functional liver at an abnormally late stage of development. A molecule that may be able to partially compensate for a loss of RALDH2 is Fgf10, which is also induced downstream of RA signaling and involved in limb and liver formation. Loss of *fgf10* prevents fin development in zebrafish,[7] and Fgf10-deficient mouse embryos lack limbs and have an abnormally small liver.[25,26] Thus, *fgf10* and *raldh2* functions may cooperate during embryogenesis such that their mutation results in similar phenotypes. Moreover, in zebrafish *fgf10* mutants, the hepatopancreatic ductal epithelium is severely dysmorphic, and cells of the hepatopancreatic ductal system and adjacent intestine misdifferentiate and adopt a hepatic or pancreatic fate.[27] These results indicate that Fgf10 functions to repress the differentiation of hepatopancreatic ductal epithelium into hepatic or pancreatic cells and thus demarcates developing organs and tissues. In our *hio* mutants, it may be that the observed lack of liver specification leads not only to impaired liver development but also to misdifferentiation in the hepatopancreatic ductal system that results in the formation of a small liver. Such misdifferentiation could obscure an absolute requirement of *raldh2* for liver specification, and might create an obstacle to finding mutations that specifically interfere with the initial specification of the liver anlage. Further analysis is needed to substantiate this hypothesis.

Comparison of* raldh2 *Alterations in Medaka* hio *and Zebrafish* nls *Mutants. The nls mutation in zebrafish is a loss-of-function allele of the *raldh2* gene that was generated by the ENU approach. Originally, *nls* was isolated in an *in situ* hybridization screen and was detected by its effects on neural AP patterning.[8] The *nls* embryos lack pectoral fin buds and fins. A similar phenotype has been reported for a natural loss-of-function *raldh2* mutation in zebrafish called *no-fin*.[10] In addition to their lack of fins, *nls* embryos do not express the hepatocyte and pancreatic cell markers that are detectable in WT zebrafish embryos.[22] Stafford and Prince[22] also showed that exogenous RA treatment of WT zebrafish embryos resulted in the anterior expansion of the pancreatic anlage. Thus, RA signaling is a determinant of the regionalization of both neuroectoderm and endoderm, and defects in *raldh2* function prevent the development of the endodermal region in which liver and pancreatic cells would normally appear. In contrast, our medaka *hio* mutation does not have severe effects on neuroectoderm and

endoderm regionalization, and the liver in *hio* embryos, although reduced in size and delayed in appearance, eventually forms in the normal location. Thus, *hio* is a unique mutation affecting liver organogenesis, and continued study of this mutation should yield new insights into the involvement of RA signaling in liver specification. It remains to be elucidated how medaka *hio* mutants escape the defect in endodermal regionalization associated with zebrafish *nls* mutations.

The availability of two closely related fish model systems, medaka and zebrafish, for studies in genetics, experimental embryology, and molecular biology is unique among vertebrates and advantageous for two reasons. First, the evolutionary distance between these two species is particularly well suited for comparative functional genomics. Second, and more importantly, the parallel existence of medaka and zebrafish transforms the perceived weakness of studying genetics in fish, namely, the many analogous groups of genes formed because of genomic duplications, into an advantage: the study of a gene in one species may shed light on a gene function that is hidden in the other species.[28] For example, RALDH2's function in AP patterning is not apparent in medaka *hio* mutants, and RALDH2's function in liver specification is not apparent in zebrafish *nls* mutants. Our results clearly demonstrate that a comparison of two related species can be a powerful means of dissecting genetic and molecular mechanisms underlying vertebrate development.

Acknowledgment: The authors thank numerous members of the Nishina and Katada laboratories for excellent fish care, technical assistance, and helpful discussions.

References

1. Zaret KS. Hepatocyte differentiation: from the endoderm and beyond. Curr Opin Genet Dev 2001;11:568-574.
2. Zaret KS. Regulatory phases of early liver development: paradigms of organogenesis. Nat Rev Genet 2002;3:499-512.
3. Furutani-Seiki M, Sasado T, Morinaga C, Suwa H, Niwa K, Yoda H, et al. A systematic genome-wide screen for mutations affecting organogenesis in Medaka, Oryzias latipes. Mech Dev 2004;121:647-658.
4. Watanabe T, Asaka S, Kitagawa D, Saito K, Kurashige R, Sasado T, et al. Mutations affecting liver development and function in Medaka, Oryzias latipes, screened by multiple criteria. Mech Dev 2004;121:791-802.
5. Hata S, Namae M, Nishina H. Liver development and regeneration: from laboratory study to clinical therapy. Dev Growth Differ 2007;49:163-170.
6. Iwamatsu T. Stages of normal development in the medaka Oryzias latipes. Mech Dev 2004;121:605-618.
7. Mercader N, Fischer S, Neumann CJ. Prdm1 acts downstream of a sequential RA, Wnt and Fgf signaling cascade during zebrafish forelimb induction. Development 2006;133:2805-2815.
8. Begemann G, Schilling TF, Rauch GJ, Geisler R, Ingham PW. The zebrafish neckless mutation reveals a requirement for raldh2 in mesodermal signals that pattern the hindbrain. Development 2001;128:3081-3094.
9. Berggren K, McCaffery P, Drager U, Forehand CJ. Differential distribution of retinoic acid synthesis in the chicken embryo as determined by immunolocalization of the retinoic acid synthetic enzyme, RALDH-2. Dev Biol 1999;210:288-304.
10. Grandel H, Lun K, Rauch GJ, Rhinn M, Piotrowski T, Houart C, et al. Retinoic acid signalling in the zebrafish embryo is necessary during pre-segmentation stages to pattern the anterior-posterior axis of the CNS and to induce a pectoral fin bud. Development 2002;129:2851-2865.
11. Mic FA, Molotkov A, Molotkova N, Duester G. Raldh2 expression in optic vesicle generates a retinoic acid signal needed for invagination of retina during optic cup formation. Dev Dyn 2004;231:270-277.
12. Niederreither K, McCaffery P, Drager UC, Chambon P, Dolle P. Restricted expression and retinoic acid-induced downregulation of the retinaldehyde dehydrogenase type 2 (RALDH-2) gene during mouse development. Mech Dev 1997;62:67-78.
13. Niederreither K, Subbarayan V, Dolle P, Chambon P. Embryonic retinoic acid synthesis is essential for early mouse post-implantation development. Nat Genet 1999;21:444-448.
14. Stratford TH, Kostakopoulou K, Maden M. Hoxb-8 has a role in establishing early anterior-posterior polarity in chick forelimb but not hindlimb. Development 1997;124:4225-4234.
15. Linville A, Gumusaneli E, Chandraratna RA, Schilling TF. Independent roles for retinoic acid in segmentation and neuronal differentiation in the zebrafish hindbrain. Dev Biol 2004;270:186-199.
16. Ng JK, Kawakami Y, Buscher D, Raya A, Itoh T, Koth CM, et al. The limb identity gene Tbx5 promotes limb initiation by interacting with Wnt2b and Fgf10. Development 2002;129:5161-5170.
17. Ober EA, Verkade H, Field HA, Stainier DY. Mesodermal Wnt2b signalling positively regulates liver specification. Nature 2006;442:688-691.
18. Shin D, Shin CH, Tucker J, Ober EA, Rentzsch F, Poss KD, et al. Bmp and Fgf signaling are essential for liver specification in zebrafish. Development 2007;134:2041-2050.
19. Morinaga C, Saito D, Nakamura S, Sasaki T, Asakawa S, Shimizu N, et al. The hotei mutation of medaka in the anti-Mullerian hormone receptor causes the dysregulation of germ cell and sexual development. Proc Natl Acad Sci U S A 2007;104:9691-9696.
20. Wakahara T, Kusu N, Yamauchi H, Kimura I, Konishi M, Miyake A, et al. Fibin, a novel secreted lateral plate mesoderm signal, is essential for pectoral fin bud initiation in zebrafish. Dev Biol 2007;303:527-535.
21. Farber SA, Pack M, Ho SY, Johnson ID, Wagner DS, Dosch R, et al. Genetic analysis of digestive physiology using fluorescent phospholipid reporters. Science 2001;292:1385-1388.
22. Stafford D, Prince VE. Retinoic acid signaling is required for a critical early step in zebrafish pancreatic development. Curr Biol 2002;12:1215-1220.
23. Wang Z, Dolle P, Cardoso WV, Niederreither K. Retinoic acid regulates morphogenesis and patterning of posterior foregut derivatives. Dev Biol 2006;297:433-445.
24. Suzuki A, Sekiya S, Buscher D, Izpisua Belmonte JC, Taniguchi H. Tbx3 controls the fate of hepatic progenitor cells in liver development by suppressing p19ARF expression. Development 2008;135:1589-1595.
25. Sekine K, Ohuchi H, Fujiwara M, Yamasaki M, Yoshizawa T, Sato T, et al. Fgf10 is essential for limb and lung formation. Nat Genet 1999;21:138-141.
26. Berg T, Rountree CB, Lee L, Estrada J, Sala FG, Choe A, et al. Fibroblast growth factor 10 is critical for liver growth during embryogenesis and controls hepatoblast survival via beta-catenin activation. HEPATOLOGY 2007;46:1187-1197.
27. Dong PD, Munson CA, Norton W, Crosnier C, Pan X, Gong Z, et al. Fgf10 regulates hepatopancreatic ductal system patterning and differentiation. Nat Genet 2007;39:397-402.
28. Furutani-Seiki M, Wittbrodt J. Medaka and zebrafish, an evolutionary twin study. Mech Dev 2004;121:629-637.
29. Lamb AL, Newcomer ME. The structure of retinal dehydrogenase type II at 2.7 A resolution: implications for retinal specificity. Biochemistry 1999;38:6003-6011.
30. Sosa-Pineda B, Wigle JT, Oliver G. Hepatocyte migration during liver development requires Prox1. Nature Genet 2000;25:254-255.

Biochemical and Biophysical Research Communications 400 (2010) 461–465

Contents lists available at ScienceDirect

Biochemical and Biophysical Research Communications

journal homepage: www.elsevier.com/locate/ybbrc

Efficiently differentiating vascular endothelial cells from adipose tissue-derived mesenchymal stem cells in serum-free culture

Masamitsu Konno [a,b], Tatsuo S. Hamazaki [a,*], Satsuki Fukuda [a], Makoto Tokuhara [a], Hideho Uchiyama [c], Hitoshi Okazawa [b], Hitoshi Okochi [a,1], Makoto Asashima [d,1]

[a] Department of Regenerative Medicine, Research Institute, National Center for Global Health and Medicine, Tokyo 162-8655, Japan
[b] Department of Neuropathology, Medical Research Institute, Tokyo Medical and Dental University, Tokyo 113-8510, Japan
[c] International Graduate School of Arts and Science, Yokohama City University, Yokohama 236-0027, Japan
[d] Department of Life Sciences (Biology), Graduate School of Arts and Sciences, The University of Tokyo, Tokyo 153-8902, Japan

ARTICLE INFO

Article history:
Received 27 July 2010
Available online 12 August 2010

Keywords:
Adipose-derived mesenchymal stem cell
Vascular endothelial cell
Differentiation
Serum-free culture
FGF2

ABSTRACT

Adipose tissue-derived mesenchymal stem cells (ASCs) have been reported to be multipotent and to differentiate into various cell types, including osteocytes, adipocytes, chondrocytes, and neural cells. Recently, many authors have reported that ASCs are also able to differentiate into vascular endothelial cells (VECs) in vitro. However, these reports included the use of medium containing fetal bovine serum for endothelial differentiation. In the present study, we have developed a novel method for differentiating mouse ASCs into VECs under serum-free conditions. After the differentiation culture, over 80% of the cells expressed vascular endothelial-specific marker proteins and could take up low-density lipoprotein in vitro. This protocol should be helpful in clarifying the mechanisms of ASC differentiation into the VSC lineage.

1. Introduction

Recently, adipose tissue is an important source of adult stem cells [1]. Adipose-derived mesenchymal stem cells (ASCs) can be obtained in high yield with minimal discomfort under local anesthesia [2,3]. After the reports of Zuk et al. [4,5], many studies have examined the plasticity, induction ability, and individual characteristics of ASCs. Derived from the embryonic mesoderm, adipose tissue is a heterogeneous cell population that includes smooth muscle cells, fibroblasts, adipocytes, mast cells, and endothelial cells [6–8]. ASCs are an adherent cell population in vitro and maintain their mesenchymal phenotype and plasticity towards the mesenchymal lineage even after they propagate in culture for several passages. These cells can differentiate into several cell types in vitro, including adipocytes, chondrocytes, osteoblasts, cardiomyocytes, and endothelial cells [5,9–13]. Moreover, ASCs are reported to have positive effects on patients who received bone marrow transplantation and suffered from GVHD (graft versus host disease), suggesting that they have an immuno-modulatory function [14].

In the present study, we focused on whether ASCs are able to differentiate into vascular endothelial cells (VECs) in a chemically defined medium after expanding them. Although mouse [15], rat [16], and human [13,17–19] ASCs have already been reported to differentiate into VECs, all of the differentiation methods have utilized fetal bovine serum (FBS). When considering the clinical applications for regenerative medicine in the future, possible contamination by animal serum is a negative factor for safety. Unknown factors in FBS also prevent researchers from accurate analysis of the differentiation mechanism. Therefore, we attempted to develop a new method for differentiating ASCs into functional VECs without serum.

2. Materials and methods

2.1. Isolation of ASCs from mice

Inguinal adipose tissue was isolated from 12- to 14-week-old adult female and GFP-transgenic C57BL/6J mice. The tissue was minced into 2–3 mm pieces in DMEM (Gibco) containing 10% FBS, and incubated at 37 °C in 5% CO_2 incubator for 1 h. Then the suspension was centrifuged at 1300 rpm for 6 min at room temperature. To dissociate the cells, they were treated with 0.12% collagenase type I solution and incubated at 37 °C for 30 min and then centrifuged at 1300 rpm for 6 min at room temperature. The cells were cultured in DMEM containing 5% FBS, 10 units penicillin,

* Corresponding author. Address: Department of Regenerative Medicine, Research Institute, National Center for Global Health and Medicine, Toyama 1-21-1, Shinjuku, Tokyo 162-8655, Japan. Fax: +81 3 3202 7192.
E-mail address: hamazaki@ri.ncgm.go.jp (T.S. Hamazaki).
[1] These authors contributed equally to this work.

0006-291X/$ - see front matter © 2010 Elsevier Inc. All rights reserved.
doi:10.1016/j.bbrc.2010.08.029

and 10 μg/ml streptomycin (GIBCO) in a CO_2 incubator at 37 °C. After continuous culture for five passages, they were used for the differentiation experiments. To eliminate any intact VECs, CD31 positive cells were removed using anti-CD31 antibody-conjugated beads (MACS) after 2 h incubation of the preparation. The CD31 negative cells were cultured and serially passaged. Animal experiments were approved by the Animal Care and Use Committee of National Center for Global Health and Medicine.

2.2. Examination of ASCs differentiation capacity into adipogenic and osteogenic differentiation

To confirm the multipotency of our cultured ASCs, we tested whether they could differentiate into adipocytes and osteoblasts, as reported previously. Passage 5 cells were cultured in adipogenic medium for 2 weeks; hMSC Adipogenic Induction SingleQuots (Cambrex) supplemented with indometacin, IBMX, insulin, dexamethasone, NCGS, and L-glutamine. The cells were fixed in 10% formalin for 10 min and stained with Oil red-O solution (Merck) to detect lipid droplets. To confirm osteogenic differentiation, the cells were cultured in osteogenic medium: hMSC Osteogenic SingleQuots (Cambrex) supplemented with ascorbate, MCGS, β-glycerophosphate, and L-glutamine. After 2 weeks, the alkaline phosphatase activity of the cells was measured by Alkaline Phosphatase Kit (Takara Bio) and the expression of an osteogenic protein marker, osteopontin, was examined by reverse transcriptase-polymerase chain reaction (RT-PCR).

2.3. Differentiation into vascular endothelial cells

To initially determine whether the ASCs could develop the characteristics of VECs or not, they were cultured in a commercially available vascular cell maintaining medium, EBM-2 (CAMBREX) containing 2% FBS and EGM-2 BulletKit (mixture of FGF2, VEGF, heparin, IGF-I, EGF, hydrocortisone, and ascorbic acid, CAMBREX) on collagen type IV coated dish, for 12 days; then their gene expression was verified. Next, we surveyed supplements that are able to replace FBS. We tested 2% KSR, B27, N2, G5, or ITS (Invitrogen); each candidate supplement was added in EBM-2 medium instead of FBS. And we also examined the other culture medium such as DMEM, IMDM, and DMEM/F12 instead of EBM-2. Finally, to determine the optimal concentration of FGF2 or VGEF, different concentrations (0, 5, 10, and 20 ng/ml) was tested for induction of endothelial cells. When the optimal culture medium for the VEC induction from ASCs was determined to be DMEM/F12 medium containing 10 ng/ml FGF2, 2% ITS, and EGM-2 BulletKit (without FGF2), further experiments for functional assay and transplantation employed this medium.

2.4. RT-PCR and real time PCR

Marker gene expression of VECs was determined by RT-PCR. After ASCs were cultured for 12 days in endothelial differentiation medium on a collagen type IV dish, total RNA was extracted by the use of Isogen (Nippon gene) as described by the manufacturer, and was treated with Superscript III (Invitrogen) to generate cDNA using oligo(dT) adaptor primer (Sigma). Then PCR amplification was performed for mouse *flk1*, *flt1*, *VE-cadherin*, and *CD31*. PCR cycles were as follows: 95 °C for 5 min, 95 °C for 30 s, annealing temperature for 30 s, 72 °C for 1 min (25–30 cycles), and 72 °C for 3 min. The RT-PCR products ware analyzed by 1% agarose gel electrophoresis and visualized with ethidium bromide. Primers for PCR were follows: *flk1* (5′-GCC AAT GAAGGG GAACTGAAGAC-3′, 5′-TCTGGCT GCTGGTGATGCTGTC-3′), *flt1* (5′-TGTGGAGAAACTTGGTGACCT-3′, 5′-TGGAGAACAGCAGGACTCCTT-3′), *ve-cadherin* (5′-TTGCCCAGCCC TACGAACCTAAAG-3′, 5′-ACCACCGCCCTCCTCATCGTAAGT-3′), *CD31* (5′-GGTGACACTGGACAAAAAGG-3′, 5′-CAGCTTCACTGCTTTGCTT G-3′), *gapdh* (5′-TGAAGGTCGGTGTGAACGGATTTGGC-3′, 5′-CATG TAGGCCATGAGGTCCACCAC-3′). For the real-time PCR, primers are follows: *tie2* (5′-GTGAAGATCAAGAATGCTACC-3′, 5′-GTGAAGATC AAGAATGCTACC-3′), *CD31* (5′-GTTTGTCAAGCGAAGGATAGATA A-3′, 5′-TCCTGCACGGTGACGTATTCACT-3′), *von Willebrand factor* (*vWF*, 5′-AACGGAAGTCCATGGTTCTG-3′, 5′-CCCCATTGAAGGCAT ACTCC-3′). Reactions were performed using SYBER Premix ExTaq (Takara Bio) and a MyiQ thermal cycler (BIORAD).

2.5. Immunocytochemistry

Differentiated endothelial-like cells from ASCs were fixed with 4% paraformaldehyde for 30 min at room temperature and then treated successively with 0.3% Triton X-100 (Wako Chemical) in PBS (Sigma) for 15 min followed by 3% bovine serum albumin (Sigma) for 30 min to reduce nonspecific reactions. The cells were reacted overnight with each of the following anti-endothelial marker antibodies at a 1:300 dilution at 4 °C; anti-flk1 (Becton Dickinson), anti-CD34 (Becton Dickinson), and anti-tie2 (Santa Cruz Biotechnology) antibodies. Then the cells were stained by Alexa Fluor 488 or 594 conjugated antibody (Molecular Probes) as the secondary antibody for 1 h at room temperature. Their nuclei were stained with DAPI for 10 min. The photographs were taken with a DP70 digital camera (Olympus) and analyzed by MetaMorph software (Molecular Devices).

2.6. Examination of cell function in vivo and in vitro

For the examination of tubular formation, the cells were seeded on Matrigel (Becton Dickinson) at 5×10^4 cells/35 mm dish. After 24 h, the morphology of the cells was examined, and phase-contrast images were photographed (Olympus IX70). For in vivo examination, the femoral muscle of a mouse was injured by liquid nitrogen and injected with the differentiated vascular endothelial-like cells (1×10^6 cells) from ASCs of GFP-transgenic mice. Two weeks after cell injection, we investigated whether the donor cells had formed vessel-like structures.

LDL uptake was assessed by incubating cells for 4 h at 37 °C with 2.5 μg/ml Alexa Fluor 488 conjugated acetyl-LDL (Molecular Probes). Cells were analyzed by fluorescence microscopy and a flow cytometer (EPICS XL, Beckman Coulter).

3. Results

3.1. In vitro differentiation of ASCs

To prove that the cultured cells from adipose tissue had retained their multipotent differentiation potential, we first confirmed that they differentiated into adipogenic and osteogenic lineages. When ASCs (Fig. 1A) were cultured in adipogenic medium for 2 weeks, more than 40% of the cells became lipid-retaining cells that stained by Oil-red O (Fig. 1B). In osteogenic medium, more than 50% of the cells were induced into an osteogenic lineage confirmed by alkaline phosphatase staining (Fig. 1C). The gene expression of *osteopontin* was also detected (Fig. 1D).

3.2. ASCs cultured in growth factor mix changed their gene expression pattern to closely resemble that of vascular endothelial cells

It was reported that the early passages of ASCs can contain small amounts of VECs and express VEC marker proteins [20]. Therefore, we used anti-CD31 antibody to remove any CD31 positive cells during the preparation of ASCs. To examine whether the ASCs could differentiate into VECs in "vascular endothelial maintaining

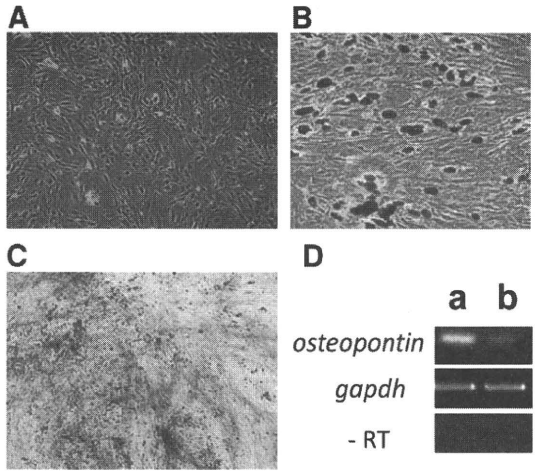

Fig. 1. Examination of mouse adipose-derived mesenchymal stem cell (ASCs) differentiation capacity into adipogenic and osteogenic lineages. (A) Mouse ASCs after five passages. (B) ASCs were cultured in adipogenic medium for 2 weeks. About 40% of the cells were stained by Oil-red O, indicating they differentiated into mature adipocytes. (C) More than 50% of the cells were positive for alkaline phosphatase staining after 2 weeks cultured in osteogenic medium, and they also express an osteopontin gene. (D) a: cultured in the osteogenic medium, b: cultured in normal ASCs medium.

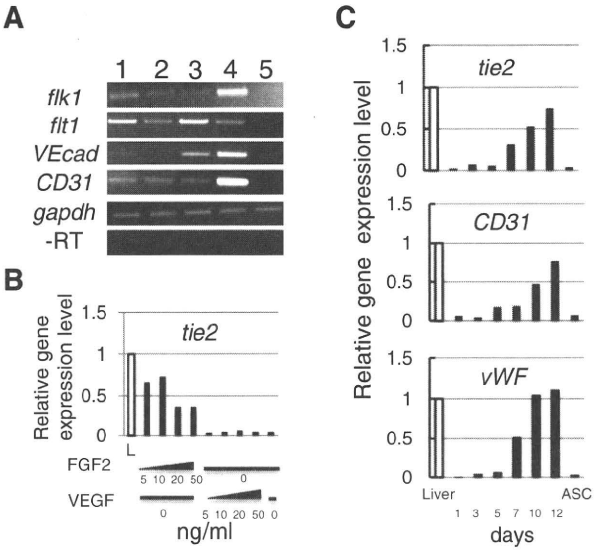

Fig. 2. Vascular endothelial-specific gene expression analyzes in different culture media. (A) RT-PCR analysis of ASCs cultured in EBM-2 medium containing EGM-2 BulletKit in the presence of FBS for 12 days (lane 1). ASCs cultured in EBM-2 containing EGM-2 BulletKit and ITS (lane 2). ASCs cultured in DMEM/F12 medium containing EGM-2 BulletKit and ITS (lane 3). Compared to the "vascular endothelial maintained medium" containing FBS (lane 1), *ve-cadherin* expression was observed almost the same level when ASCs cultured in serum-free DMEM/F12 medium (lane 3). For comparison, 8-week-old mouse liver cells (lane 4) and normal ASCs (lane 5) are shown. (B) Effects of FGF2 and VEGF in different concentrations on the differentiation of ASCs Expression of *tie2*, one of the vascular endothelial markers, was highest when 10 ng/ml FGF2 containing medium was used. *Tie2* gene expression did not elevate in any concentrations of VEGF in the absence of FGF2 and serum L (liver used as positive control). (C) Time course expression of *tie2*, *CD31*, and *vWF* genes. All of genes were upregulated 7–10 days after the beginning of differentiation culture. ASCs were differentiated in DMEM/F12 medium containing EGM-2 BulletKit (without FGF2), ITS, and 10 ng/ml FGF-2.

medium", we cultured ASCs in EBM-2 medium containing 2% FBS and EGM-2 BulletKit on a collagen type IV coated dish. After 12 days of culture, they expressed the vascular endothelial marker genes, *flk1, flt1, ve-cadherin*, and *CD31* (Fig. 2A, lane 1). Normal ASCs did not express these genes at all (Fig. 2A, lane 5). These results indicate that the ASCs have capacity to differentiate into VECs. The "vascular endothelial maintaining medium" contains 2% FBS, which may contain variable amounts of unknown factors including growth factors. To establish a stable method for differentiating VECs from ASCs, we tried to establish a serum-free culture method. We tested 2% KSR, B27, N2, G5, and ITS as replacements for FBS and found that the ITS supplement (insulin, transferrin, and selenium) had almost the same effects as FBS on endothelial differentiation. The cells expressed *flk1, flt1* and *CD31* but did not express *ve-cadherin* (Fig. 2A, lane 2). Others supplements were not so much upregulated the gene expressions except for ITS (data not shown). Therefore, we tested other types of basal medium, DMEM, IMDM, and DMEM/F12, as replacements for EBM-2. When we changed the medium from EBM-2 to DMEM/F12, the gene expression of *ve-cadherin* was proven (Fig. 2A, lane 3). There was no effect was observed when the medium was used DMEM or IMDM (data not shown).

Next, we attempted to determine the optimal concentrations of FGF2 and VEGF, because both factors are considered to be important for the differentiation of VECs [21,22]. The ASCs were seeded in DMEM/F12 medium containing ITS and EGM-2 Bulletkit (without FGF2 and VEGF). Then we added various concentrations of FGF2 or VEGF to the culture medium. After 12 days, we analyzed for expression of the early vascular endothelial marker gene, *tie2*, by real-time PCR. Without FGF2, expressions of vascular endothelial marker genes did not increase (Fig. 2B) even when the concentration of VEGF was elevated. On the other hand, in the presence of FGF2, *tie2* expression level increased, and 10 ng/ml FGF2 was the most efficient concentration (Fig. 2B). These results indicate that, when the ASCs differentiate into VECs in this serum-free medium, FGF2 plays a more important role than VEGF.

When we examined the time course expression of vascular endothelium-specific genes of ASCs cultured in this differentiation medium, *tie2* and *CD31* showed almost the same pattern of expression, beginning to express after 5–7 days culture and increasing gradually up to 12 days. Gene expression of *vWF* increased after 7 days culture and reached almost its highest level after 10 days culture (Fig. 2C).

It must be mentioned that we used two lines of ASCs prepared differently during primary culture; one was prepared directly without any selection and the other was the cell population from which CD31 positive cells were removed to avoid contamination by intact endothelial cells. After five passages, both lines were examined for vascular endothelial differentiation, no differences between the two groups with respect to the differentiation efficiency were detected.

3.3. Differentiated ASCs express vascular endothelial-specific protein

To examine whether the differentiated ASCs actually expressed vascular endothelial-specific marker proteins, we stained those cells with anti-flk1, anti-tie2, and anti-CD34 antibodies. Most of the cells positively expressed flk1, tie2, and CD34 (Fig. 3A–C). The average of percentages of positive cells calculated by MetaMorph software were as follows: flk1 (82%), tie2 (78%), and CD34 (87%), respectively. These results indicate that approximately 80–90% of the ASCs differentiated into vascular endothelial-like cells.

3.4. VECs differentiated from ASCs showed similar morphological and physiological functions in vitro and in vivo

After ASCs were cultured in DMEM/F12 medium with EGM-2 BulletKit (without FGF2), ITS and 10 ng/ml FGF2 on collagen type IV coated dishes, they were capable of forming tubular-like vascular structures when they were seeded in Matrigel dishes (Fig. 4C). In contrast, ASCs cultured in DMEM containing 5% FBS

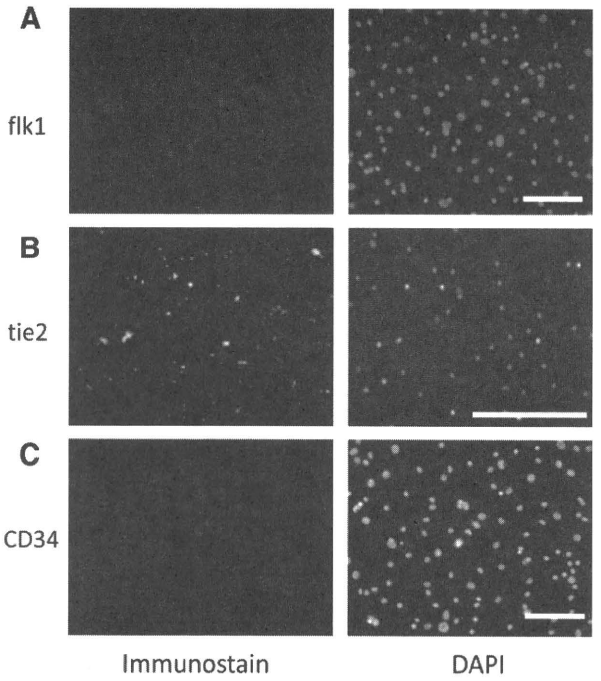

Fig. 3. Immunohistochemical staining of differentiated ASCs with anti-vascular endothelial marker proteins antibodies. All of three marker proteins (flk1, tie2, and CD34) were positively stained against the differentiated ASCs cultured for 12 days in the medium. Calculated with Metamorph software, average of flk1 (A), tie2 (B), and CD34 (C) positive cells were about 82%, 78%, and 87%, respectively ($n = 6$). Nuclei were stained with DAPI. Scale bar, 200 μm.

did not form such structures (Fig. 4A and B). We next examined whether the differentiated cells formed vessel-like structures in vivo. The femoral muscle of a C57BL/6J mouse was injured by liquid nitrogen. Then we injected vascular endothelial-like cells that had differentiated from ASCs derived from GFP mice into the muscle. Two weeks after the injection, we analyzed tissue samples to determine whether the cells histologically contribute to vessel-like structures. We found that GFP positive cells were incorporated into vessel-like structures, indicating that the VECs which were differentiated from ASCs successfully formed these structures (Fig. 4D) but control cells which cultured in DMEM medium containing 5% FBS did not (data not shown). These results suggest that the induced ASCs were able to form tubular structures almost as well as intact endothelial cells in vitro and in vivo.

Finally, we examined the efficiency of differentiation of ASCs into VECs by measuring LDL uptake. Alexa Flour 488-conjugated acetyl-LDL was added to the medium, and fluorescence positive cells were counted by a flow cytometer and observed under a fluorescence microscope. The differentiated ASCs showed very high acetyl-LDL uptake; over 80% of the cells were fluorescence positive (Fig. 4E and F). Undifferentiated ASCs did not uptake acetyl-LDL at all (Fig. 4F).

4. Discussion

In the present study, we showed that mouse ASCs can differentiate into VECs in serum-free medium in vitro. They formed tubular structures in Matrigel culture, and contributed to vessel-like structures in vivo. Analysis of the vascular endothelial function revealed that over 80% of cells incorporated acetyl-LDL during 6 h of culture, indicating most of the cells differentiated into the functional VECs. These results indicate our differentiation method can be useful for the efficient differentiation of VECs from ASCs.

It is well known that early passage ASCs contain VECs. However, these VECs are also reported to disappear when ASCs are continuously cultured until passage 5 [20], indicating that the VECs in adipose tissue do not propagate in the culture medium for ASCs. To rule out the possibility that VECs were contaminating our ASCs, (i) we removed the VECs using anti-CD31 antibody-conjugated beads before the primary culture and (ii) we used ASCs cultured for more than five passages. Both of the cell population almost equally differentiated into VECs; and there was no detectable difference. These results suggest that most of the intact VECs that may exist in a large population of ASCs at first disappear during continuous culture and propagation of ASCs.

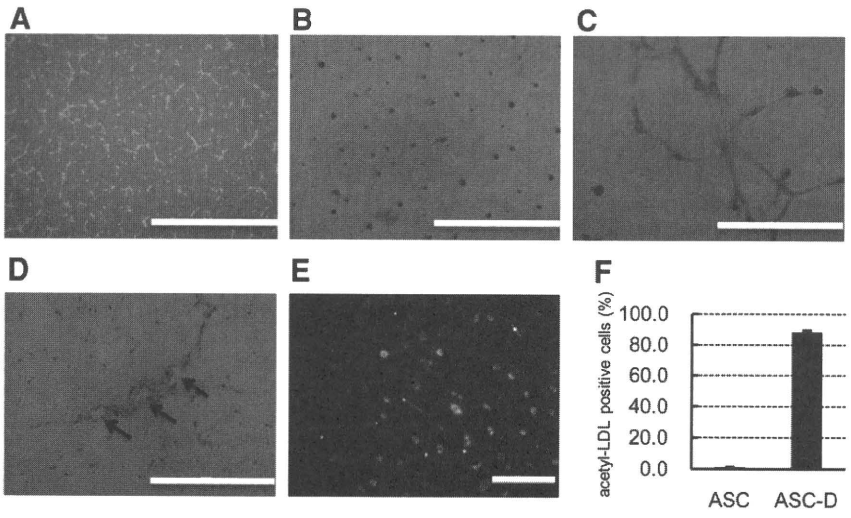

Fig. 4. Morphological and physiological functions of differentiated ASCs. Morphological changes in vascular endothelial-like cells differentiated from ASCs were examined. (A) Normal ASCs were cultured in matrigel for 6 h (A) and 24 h (B). Tubular formation was observed when vascular endothelial-like cells differentiated from ASCs were cultured in matrigel for 24 h (C). Vessel-like structures were formed in the mouse muscle and injected EGFP positive donor cells (brown and arrows) participated in the vessels (D). Acetyl-LDL conjugated fluorescence uptake of differentiated ASCs was examined. Most of the differentiated ASCs were green fluorescence positive when they were cultured in DMEM/F12 medium containing EGM-2 Bulletkit (without FGF2), ITS, and 10 ng/ml FGF2 for 12 days (E). (F) A flow cytometry analysis showed that more than 85% of the differentiated cells (ASC-D) incorporated acetyl-LDL. Normal ASCs did not acetyl-LDL uptake at all (ASC). Scale bar, 2 mm (A–C) and 200 μm (D and E).

FGF2 is a critical growth factor for the induction of VECs. It is reported to play an important role on angiogenesis and vasculogenesis [23–25]. VEGF is also reported to be a key growth factor during embryonic development and differentiation of vascular system [22,26]. We attempted to determine how important and effective these factors are for the induction of VECs in our serum-free condition. We examined the optimal concentrations of these growth factors and demonstrated that the presence of FGF2 upregulated the gene expression of vascular endothelial markers. Therefore, in serum-free conditions, FGF2 is considered an essential growth factor for ASC differentiation into VSC. It is reported that the biologic activity of FGF2 is dependent on the presence of heparin. Small heparin oligosaccharides of defined sizes can activate the mitogenic potential of FGF2 on appropriate target cells and are active in the binding of FGF2 to a soluble FGF2 receptor [27,28]. In the present study, the culture medium contains heparin and it probably upregulates the activity of FGF2. It is possible that heparin plays a critical role in the differentiation from ASCs into VECs in the absence of serum. One the other hand, VEGF did not influence the *tie2* gene expression at any concentration (Fig. 2B) when the culture medium did not contain FGF2. VEGF is reported to be secreted by both mouse [29] and human [30] cultured ASCs, and VEGF expression of VECs is induced by FGF2 [31]. Therefore, additional supplementation with VEGF was not effective for differentiation of VECs in the absence of FGF2 in our experiments.

ASCs were reported to differentiate into VECs when they were cultured in a medium containing FBS [15–18]. FBS contains various unknown factors in varying amounts and may prevent further analysis of the differentiation mechanisms. It is also a negative when cells are prepared for clinical use, because the cells could possibly incorporate proteins or carbohydrates derived from this [32]. The present study intended to establish a medium for differentiation from ASCs to VECs without the usage of FBS. Our method is useful for further analysis of the mechanisms of differentiation from ASCs to VECs and will shed new light on stem cell research.

Acknowledgments

We are grateful to Dr. Barbara Lee Smith Pierce (University of Maryland University College) for editorial work in the preparation of this manuscript. This work was supported by a Grant for National Center for Global Health and Medicine (21A114) and by the grant for Organ Regeneration Project, International Cooperative Research Program, Japan Science and Technology Agency.

Appendix A. Supplementary data

Supplementary data associated with this article can be found, in the online version, at doi:10.1016/j.bbrc.2010.08.029.

References

[1] S. Hombach-Klonisch, S. Panigrahi, I. Rashedi, A. Seifert, E. Alberti, P. Pocar, M. Kurpisz, K. Schulze-Osthoff, A. Mackiewicz, M. Los, Adult stem cells and their trans-differentiation potential—perspectives and therapeutic applications, J. Mol. Med. 86 (2008) 1301–1314.
[2] L. Casteilla, C. Dani, Adipose tissue-derived cells: from physiology to regenerative medicine, Diabetes Metab. 32 (2006) 393–401.
[3] F. D'Andrea, F. De Francesco, G.A. Ferraro, V. Desiderio, V. Tirino, A. De Rosa, G. Papaccio, Large-scale production of human adipose tissue from stem cells: a new tool for regenerative medicine and tissue banking, Tissue Eng. Part C Methods 14 (2008) 233–242.
[4] P.A. Zuk, M. Zhu, P. Ashjian, D.A. De Ugarte, J.I. Huang, H. Mizuno, Z.C. Alfonso, J.K. Fraser, P. Benhaim, M.H. Hedrick, Human adipose tissue is a source of multipotent stem cells, Mol. Biol. Cell 13 (2002) 4279–4295.
[5] P.A. Zuk, M. Zhu, H. Mizuno, J. Huang, J.W. Futrell, A.J. Katz, P. Benhaim, H.P. Lorenz, M.H. Hedrick, Multilineage cells from human adipose tissue: implications for cell-based therapies, Tissue Eng. 7 (2001) 211–228.
[6] G.J. Hausman, Techniques for studying adipocytes, Stain Technol. 56 (1981) 149–154.
[7] G.J. Hausman, D.R. Campion, Histology of the stroma in developing rat subcutaneous adipose tissue, J. Anim. Sci. 55 (1982) 1336–1342.
[8] P. Pettersson, M. Cigolini, L. Sjostrom, U. Smith, P. Bjorntorp, Cells in human adipose tissue developing into adipocytes, Acta Med. Scand. 215 (1984) 447–451.
[9] Y.C. Halvorsen, W.O. Wilkison, J.M. Gimble, Adipose-derived stromal cells—their utility and potential in bone formation, Int. J. Obes. Relat. Metab. Disord. 24 (Suppl. 4) (2000) S41–S44.
[10] Y.D. Halvorsen, D. Franklin, A.L. Bond, D.C. Hitt, C. Auchter, A.L. Boskey, E.P. Paschalis, W.O. Wilkison, J.M. Gimble, Extracellular matrix mineralization and osteoblast gene expression by human adipose tissue-derived stromal cells, Tissue Eng. 7 (2001) 729–741.
[11] M.K. Majumdar, V. Banks, D.P. Peluso, E.A. Morris, Isolation, characterization, and chondrogenic potential of human bone marrow-derived multipotential stromal cells, J. Cell. Physiol. 185 (2000) 98–106.
[12] V. Planat-Benard, J.S. Silvestre, B. Cousin, M. Andre, M. Nibbelink, R. Tamarat, M. Clergue, C. Manneville, C. Saillan-Barreau, M. Duriez, A. Tedgui, B. Levy, L. Penicaud, L. Casteilla, Plasticity of human adipose lineage cells toward endothelial cells: physiological and therapeutic perspectives, Circulation 109 (2004) 656–663.
[13] S. Rangappa, C. Fen, E.H. Lee, A. Bongso, E.K. Sim, Transformation of adult mesenchymal stem cells isolated from the fatty tissue into cardiomyocytes, Ann. Thorac. Surg. 75 (2003) 775–779.
[14] E. Lombardo, O. DelaRosa, P. Mancheno-Corvo, R. Menta, C. Ramirez, D. Buscher, Toll-like receptor-mediated signaling in human adipose-derived stem cells: implications for immunogenicity and immunosuppressive potential, Tissue Eng. Part A 15 (2009) 1579–1589.
[15] H. Nakagami, R. Morishita, K. Maeda, Y. Kikuchi, T. Ogihara, Y. Kaneda, Adipose tissue-derived stromal cells as a novel option for regenerative cell therapy, J. Atheroscler. Thromb. 13 (2006) 77–81.
[16] H. Ning, G. Liu, G. Lin, R. Yang, T.F. Lue, C.S. Lin, Fibroblast growth factor 2 promotes endothelial differentiation of adipose tissue-derived stem cells, J. Sex. Med. 6 (2009) 967–979.
[17] Y. Cao, Z. Sun, L. Liao, Y. Meng, Q. Han, R.C. Zhao, Human adipose tissue-derived stem cells differentiate into endothelial cells in vitro and improve postnatal neovascularization in vivo, Biochem. Biophys. Res. Commun. 332 (2005) 370–379.
[18] J. Oswald, S. Boxberger, B. Jorgensen, S. Feldmann, G. Ehninger, M. Bornhauser, C. Werner, Mesenchymal stem cells can be differentiated into endothelial cells in vitro, Stem Cells 22 (2004) 377–384.
[19] V. Planat-Benard, C. Menard, M. Andre, M. Puceat, A. Perez, J.M. Garcia-Verdugo, L. Penicaud, L. Casteilla, Spontaneous cardiomyocyte differentiation from adipose tissue stroma cells, Circ. Res. 94 (2004) 223–229.
[20] D.O. Traktuev, S. Merfeld-Clauss, J. Li, M. Kolonin, W. Arap, R. Pasqualini, B.H. Johnstone, K.L. March, A population of multipotent CD34-positive adipose stromal cells share pericyte and mesenchymal surface markers, reside in a periendothelial location, and stabilize endothelial networks, Circ. Res. 102 (2008) 77–85.
[21] C. Basilico, D. Moscatelli, The FGF family of growth factors and oncogenes, Adv. Cancer Res. 59 (1992) 115–165.
[22] N. Ferrara, K. Carver-Moore, H. Chen, M. Dowd, L. Lu, K.S. O'Shea, L. Powell-Braxton, K.J. Hillan, M.W. Moore, Heterozygous embryonic lethality induced by targeted inactivation of the VEGF gene, Nature 380 (1996) 439–442.
[23] I. Flamme, W. Risau, Induction of vasculogenesis and hematopoiesis in vitro, Development 116 (1992) 435–439.
[24] J. Folkman, C. Haudenschild, Angiogenesis in vitro, Nature 288 (1980) 551–556.
[25] A. Kurane, N. Vyavahare, In vivo vascular tissue engineering: influence of cytokine and implant location on tissue specific cellular recruitment, J. Tissue Eng. Regen. Med. 3 (2009) 280–289.
[26] P. Carmeliet, V. Ferreira, G. Breier, S. Pollefeyt, L. Kieckens, M. Gertsenstein, M. Fahrig, A. Vandenhoeck, K. Harpal, C. Eberhardt, C. Declercq, J. Pawling, L. Moons, D. Collen, W. Risau, A. Nagy, Abnormal blood vessel development and lethality in embryos lacking a single VEGF allele, Nature 380 (1996) 435–439.
[27] D.M. Ornitz, A. Yayon, J.G. Flanagan, C.M. Svahn, E. Levi, P. Leder, Heparin is required for cell-free binding of basic fibroblast growth factor to a soluble receptor and for mitogenesis in whole cells, Mol. Cell. Biol. 12 (1992) 240–247.
[28] A. Yayon, M. Klagsbrun, J.D. Esko, P. Leder, D.M. Ornitz, Cell surface, heparin-like molecules are required for binding of basic fibroblast growth factor to its high affinity receptor, Cell 64 (1991) 841–848.
[29] S. El-Ftesi, E.I. Chang, M.T. Longaker, G.C. Gurtner, Aging and diabetes impair the neovascular potential of adipose-derived stromal cells, Plast. Reconstr. Surg. 123 (2009) 475–485.
[30] J. Rehman, D. Traktuev, J. Li, S. Merfeld-Clauss, C.J. Temm-Grove, J.E. Bovenkerk, C.L. Pell, B.H. Johnstone, R.V. Considine, K.L. March, Secretion of angiogenic and antiapoptotic factors by human adipose stromal cells, Circulation 109 (2004) 1292–1298.
[31] G. Seghezzi, S. Patel, C.J. Ren, A. Gualandris, G. Pintucci, E.S. Robbins, R.L. Shapiro, A.C. Galloway, D.B. Rifkin, P. Mignatti, Fibroblast growth factor-2 (FGF-2) induces vascular endothelial growth factor (VEGF) expression in the endothelial cells of forming capillaries: an autocrine mechanism contributing to angiogenesis, J. Cell. Biol. 141 (1998) 1659–1673.
[32] M.J. Martin, A. Muotri, F. Gage, A. Varki, Human embryonic stem cells express an immunogenic nonhuman sialic acid, Nat. Med. 11 (2005) 228–232.

GASTROENTEROLOGY 2010;138:1525–1535

BASIC—LIVER, PANCREAS, AND BILIARY TRACT

Characterization and Functional Analyses of Hepatic Mesothelial Cells in Mouse Liver Development

IZUMI ONITSUKA,* MINORU TANAKA,*,‡ AND ATSUSHI MIYAJIMA*

*Laboratory of Cell Growth and Differentiation and ‡Promotion of Independence for Young Investigators, Institute of Molecular and Cellular Biosciences, University of Tokyo, Tokyo, Japan

BACKGROUND & AIMS: At the onset of liver development, cardiac mesoderm, septum transversum mesenchyme, and endothelial cells are involved in the specification and/or proliferation of hepatoblasts. After this initial stage, however, it is unclear which cells support the proliferation and differentiation of hepatocytes. Here we characterized the nature of mouse hepatic mesothelial cells (MCs) and investigated their role in organogenesis. **METHODS:** Using anti-podocalyxin-like protein 1 (PCLP1) and anti-mesothelin antibodies, we characterized MCs during liver development by immunohistochemistry, flow cytometry, and gene expression analysis. The possible role of MCs in hepatogenesis was investigated by in vitro culture and analysis of Wilms' tumor 1 homologue (WT1) knockout mice. **RESULTS:** PCLP1 was highly expressed in immature MCs, covering the surface of lobes. PCLP1 expression in MCs was down-regulated along with development, whereas mesothelin expression was up-regulated, indicating that these molecules distinguished developmental stages of MCs. The proliferation potential of MCs was high in the fetus and declined after birth. Fetal MCs expressed various growth factors and strongly enhanced the expansion of fetal hepatocytes in vitro, whereas differentiated MCs exhibited less growth factor expression, and differentiated MCs failed to enhance hepatocyte proliferation in vitro. In WT1-deficient embryos, hepatocyte proliferation was impaired due to defective MCs. **CONCLUSIONS: The mesothelium is not only an inert protective sheet covering the parenchyma but also changes its characteristics dynamically during development and plays an active role in organogenesis by promoting expansion of parenchymal cells.**

Keywords: Mesothelium; Mesothelin; Podocalyxin-Like Protein 1; Cell Sorting.

In mouse liver development, hepatic cells are induced from the embryonic endoderm by embryonic day (E) 8.5. The cardiac mesoderm and septum transversum mesenchyme (STM) adjacent to the foregut endoderm produce fibroblast growth factors and bone morphogenetic protein, respectively, to induce liver specification.[1,2] Thereafter, the specified endodermal cells, hepatoblasts, outgrow into the STM to form hepatic cords by the support of endothelial cells (ECs).[3] However, the mechanism of liver development after the liver bud formation remains largely unknown. Although various cytokines have been shown to stimulate proliferation of hepatocytes in vitro (eg, epidermal growth factor, hepatocyte growth factor [HGF], and pleiotrophin [Ptn]),[4,5] it remains elusive how hepatocyte proliferation is supported by surrounding cells in vivo. The lack of tools to precisely identify and isolate different types of liver cells has hampered such investigation. Suksaweang et al have shown that proliferation of hepatocytes is limited to the peripheral region of the hepatic lobe during liver development in the chick.[6] They also suggested that mesenchymal cells located at the periphery of the lobe might provide the microenvironment for hepatocytes to proliferate.[6] However, it was unclear which peripheral mesenchymal cells contribute to hepatogenesis during liver development.

In vertebrates, the periphery of all coelomic organs is covered by a single layer of mesothelial tissue, which provides nonadhesive and protective surfaces. The mesothelium is derived from the lateral plate mesoderm and is believed to play an important role in maintaining normal serosal integrity and functions, such as transport

Abbreviations used in this paper: Ab, antibody; bFGF, basic fibroblast growth factor; Dlk1, delta-like 1 homologue; E, embryonic day; EC, endothelial cell; HGF, hepatocyte growth factor; IHC, immunohistochemistry; MC, mesothelial cell; Mdk, midkine; Msln, mesothelin; OSM, oncostatin M; PCLP1, podocalyxin-like protein 1; PCR, polymerase chain reaction; PD, postnatal day; Ptn, pleiotrophin; RALDH2, retinaldehyde dehydrogenase; RT, reverse-transcription; STM, septum transversum mesenchyme; WT1, Wilms' tumor 1 homologue.

0016-5085/10/$36.00
doi:10.1053/j.gastro.2009.12.059

of fluid and cells in serosal cavities, antigen presentation, inflammation, and tissue repair.[7] During vertebrate development, recent studies have shown that splanchnic mesothelial cells (MCs) delaminate into the parenchymal region and give rise to the vascular cells and mesenchymal cells in multiple coelomic organs, including murine heart,[8] lung,[9] gut,[10] and avian liver.[11] These observations suggest that splanchnic MCs might play important roles in organogenesis as a source of vascular and/or mesenchymal cells in multiple organs. Despite these accumulating reports, however, the precise characteristics of MCs and their roles for the development of parenchymal cells remain largely unknown.

In this study, we show that podocalyxin-like protein 1 (PCLP1) and mesothelin (Msln) are excellent markers to identify and isolate hepatic MCs. PCLP1 is a member of the sialomucin family and was originally identified as a protein highly expressed on glomerular podocytes in avian and mammalian kidneys.[12] It was also reported that PCLP1 is expressed on ECs,[13] immature mesodermal cells such as hemangioblasts, the common progenitor for hematopoietic and vascular endothelial cells,[14] and hematopoietic stem cells.[15] Msln is a glycosylphosphatidylinositol-linked glycoprotein highly expressed in a variety of normal mesothelial tissues, mesotheliomas, and ovarian cancers.[16] Using these cell surface markers, we characterize MCs and show that fetal hepatic MCs are a rich source of multiple growth factors for hepatocytes from early to late stages in liver development, indicating that MC layers play an active role in organogenesis.

BASIC-LIVER, PANCREAS, AND BILIARY TRACT

Materials and Methods

Mice

C57BL/6 mice were purchased from Nihon SLC (Hamamatsu, Japan). Mice were maintained and mated in the institutional animal facility according to the guidelines of the University of Tokyo. The time at midday (12:00) was taken to be E0.5 for plugged mice. WT1 knockout mice[17] were kindly provided by Dr R. Nishinakamura. Embryos were genotyped by polymerase chain reaction (PCR).

Cell Preparation for Flow Cytometric Analysis and Sorting

Livers isolated from embryos were dissociated into a single-cell suspension and stained by antibodies according to the previous report.[18] Cells were analyzed by FACSCalibur (BD Biosciences) or EPICS ALTRA (Beckman Coulter, San Diego, CA). For cell sorting, EPICS ALTRA or autoMACS (Miltenyi Biotec K.K., Tokyo, Japan) instruments were used. Purity of the sorted cell populations estimated by flow cytometry was higher than 90%.

Expansion of Fetal Hepatic MCs and Coculture With Hepatoblasts

Flk1$^-$PCLP1^{high} cells were sorted from E12.5 livers by a cell sorter and expanded in vitro on type IV collagen-coated dishes in α-minimum essential medium containing 10% fetal bovine serum and 50 nmol/L mercaptoethanol, 10 ng/mL oncostatin M (OSM), and 10 ng/mL basic fibroblast growth factor (bFGF). For passage, cells were trypsinized with 0.05% trypsin and 0.5 mmol/L EDTA (Sigma-Aldrich, St. Louis, MO) in phosphate-buffered saline at 37°C for 8 minutes and replated. Delta-like 1 homologue (Dlk1$^+$) fetal hepatoblasts were purified from E14.5 livers using autoMACS as reported previously. A total of 2×10^3 Dlk1$^+$ cells were inoculated into each well of a gelatin-coated 24-well plate with α-minimum essential medium containing 10% fetal bovine serum with or without 1×10^5 in vitro expanded fetal hepatic MCs, which were separated in a 3.0-μm pored Transwell (Corning, NY). As a positive control for proliferation, 25 ng/mL pleiotrophin (Ptn) or 50 ng/mL midkine (Mdk) was added to the culture. After 3 days of culture, cells were stained with Giemsa solution to visualize the colonies or subjected to WST-1 assay (Roche, Diagnostics KK, Tokyo, Japan) according to the manufacturer's protocol. Averages in triplicate cultures were used to determine cell proliferation.

Results

PCLP1 Is Highly Expressed on the Surface Layers of Multiple Coelomic Organs During Embryogenesis

It was reported previously that PCLP1 is widely expressed by "boundary elements," including vasculature, mesothelial linings, and the luminal surface of newly formed cavities in murine embryos.[15] Immunohistochemistry (IHC) of embryonic sections with anti-PCLP1 antibody (Ab) showed that PCLP1 was expressed highly on the surface of multiple coelomic organs such as heart, lung, liver, and stomach (data not shown). Because all the coelomic organs are covered by a single layer of MCs, cells with an intense PCLP1 signal were suggested to be the mesothelial lining.

On E9.5 tissue sections, double staining with anti-PCLP1 Ab and anti-Dlk1 Ab, which recognizes fetal hepatoblasts,[18,19] showed the presence of PCLP1$^+$ cells in the STM, where hepatic cords form with Dlk1$^+$ hepatoblasts emerging from the foregut endoderm (Figure 1*A*). At E10.5, a monolayer of cells with an intense PCLP1 signal was detected on the surfaces of dorsal lobes, and these cells covered each hepatic lobe completely at E12.5 (Figure 1*A*). While the signals were continuously detected at E16.5, their frequency and intensity were reduced at postnatal day (PD) 4, and no PCLP1 signal was detected on the surface of adult livers (Figure 1*A*). These results suggested that the PCLP1 expression on the surface of hepatic lobes is regulated in a stage-specific manner. By

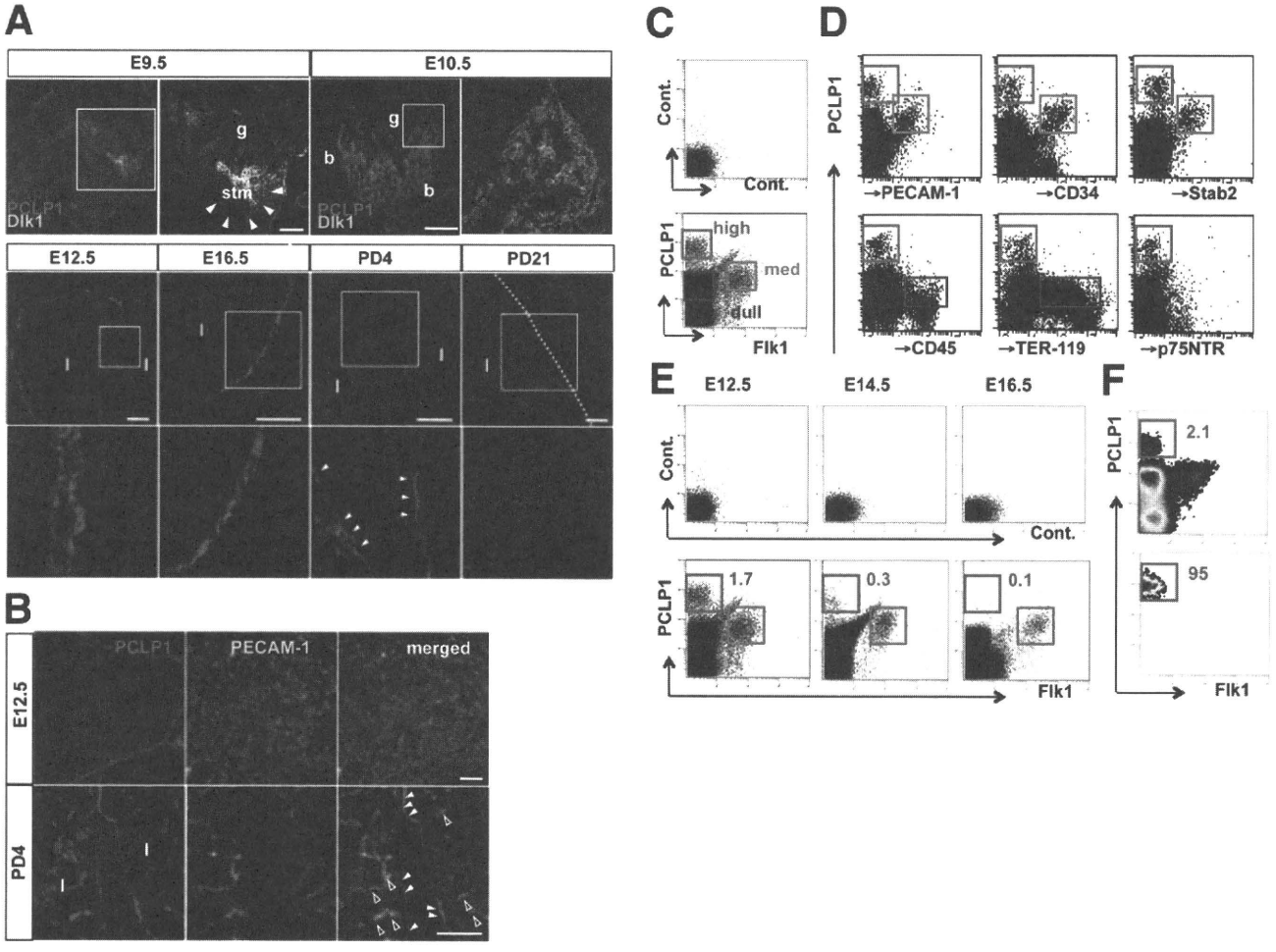

Figure 1. IHC and flow cytometry with anti-PCLP1 Ab in the developing liver. (*A* and *B*) IHC with anti-PCLP1 (*red*), anti-Dlk1 (*green* in *A*), and anti–PECAM-1 (*green* in *B*) Abs and 4′,6-diamidino-2-phenylindole (*blue* in *A*). Higher-magnification images of the *boxed regions* in *A* are shown to the right (E9.5 and E10.5) or underneath (E12.5 to PD21). The *dotted line* in *A* (PD21) delineates the periphery of the hepatic lobe. *Arrowheads* indicate PCLP1^{+} cells in the STM region (E9.5) or in the mesothelial layer (PD4 in *A* and *B*), respectively. *Open arrowheads* in *B* indicate PECAM1^{+}PCLP1^{med} sinusoidal ECs. g, gut; stm, septum transversum mesenchyme; b, body wall; l, lobe. *Scale bars* = 100 μm. (*C*) Flow cytometry of E12.5 liver cells using anti-PCLP1 and anti-Flk1 Abs. *Red*, *green*, and *blue lines* in the *lower panel* indicate Flk1^{-}PCLP1^{high}, Flk1^{+}PCLP1^{med}, and Flk1^{-}PCLP1^{dull} cell populations, respectively. (*D*) Flow cytometry of E12.5 liver cells using anti-PCLP1 Ab and other cell surface molecules. *Red*, *green*, and *blue lines* in each *panel* indicate PCLP1^{high}, PCLP1^{med}, and PCLP1^{dull} cell populations, respectively. (*E*) Flow cytometry of E12.5, E14.5, and E16.5 liver cells using anti-PCLP1 and anti-Flk1 Abs. *Red* and *green lines* in each *lower panel* indicate Flk1^{-}PCLP1^{high} and Flk1^{+}PCLP1^{med} cells, respectively. The number indicates the percentage of Flk1^{-}PCLP1^{high} cells. (*F*) Flow cytometry of E12.5 liver cells before (*upper panel*) and after (*lower panel*) sorting of Flk1^{-}PLCP1^{high} cells by a cell sorter. Sorting gates are indicated by *red lines*. Numbers in each *panel* indicate the percentage of Flk1^{-}PCLP1^{high} cells.

contrast, weak PCLP1 signals were observed in the parenchymal region from E12.5 to adults. In accordance with the previous report that PCLP1 is expressed on ECs,[13] weak PCLP1 signals colocalized with PECAM-1, an endothelial marker, in the parenchymal region; however, no colocalization occurred with strong PCLP1 signals in the mesothelial lining (Figure 1*B*).

Flow Cytometric Analysis of PCLP1^{+} Cells in Fetal Liver

Flow cytometry of E12.5 fetal liver cells with anti-PCLP1 Ab and anti-Flk1 Ab, which detects ECs, revealed that PCLP1^{+} cells could be fractionated into at least 3 populations, PCLP1^{high}, PCLP1^{med}, and PCLP1^{dull} cells, based on the expression levels of PCLP1 (Figure 1*C*). Multicolor flow cytometry revealed that PCLP1^{med} cells were positive for several EC markers but not for CD45 (Figure 1*D* and data not shown). PCLP1^{dull} cells contained TER-119^{+} erythroids and CD45^{+} leukocytes (Figure 1*D*), consistent with the previous report.[15] By contrast, PCLP1^{high} cells were completely negative for EC and blood cell markers as well as the hepatic stellate cell marker p75 neurotrophin receptor[20] (Figure 1*C*–*E*), indicating that the Flk1^{-}PCLP1^{high} cell population was distinct from these nonparenchymal cells. The fraction of Flk1^{-}PCLP1^{high} cells in total fetal liver cells decreased as development progressed (Figure 1*E*).

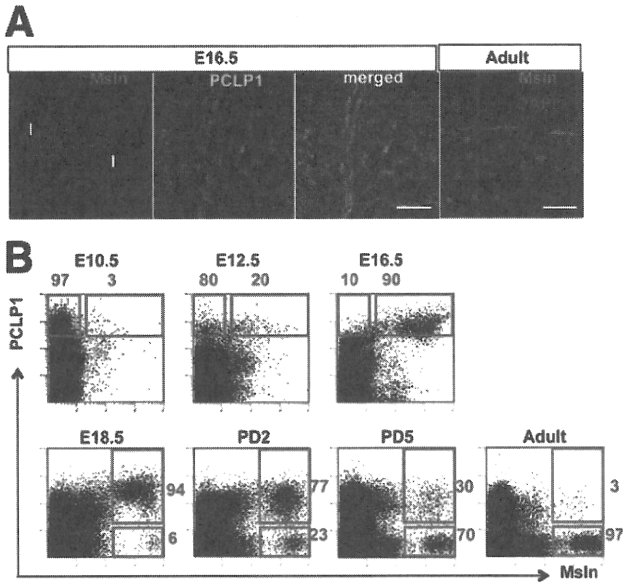

Figure 2. Expression of PCLP1 and Msln in the mesothelial layer during liver development. (*A*) IHC of liver sections with anti-Msln (*red*) and anti-PCLP1 (*green*) Abs. l, lobe. *Scale bars* = 80 μm. (*B*) Flow cytometry of liver cells with anti-PCLP1 and anti-Msln Abs. *Red lines* in each panel indicate PCLP1^{high} (*upper panels*) and Msln^{+} (*lower panels*) cell populations, respectively. The cells of whole livers (E10.5 and E12.5) and surgically separated mesothelial tissues (E16.5, E18.5, PD2, PD5, and Adult) were used for flow cytometry. Numbers in each *panel* indicate the percentage of each cell population in PCLP1^{high} (*upper panels*) or in Msln^{+} (*lower panels*) cells.

Flow cytometry of surgically separated E16.5 livers into mesothelial and nonmesothelial tissues under a stereomicroscope revealed that Flk1^{-}PCLP1^{high} cells were present exclusively in the mesothelial tissue, while Flk1^{+}PCLP1^{med} cells were detected mainly in the nonmesothelial tissue (Supplementary Figure 1*A* and *B*). These results indicated that the PCLP1^{high} and PCLP1^{med} cells by flow cytometry correspond to fetal MCs and ECs detected by IHC, respectively, and that PCLP1^{high} cells could be isolated by a cell sorter with high purity (Figure 1*F*).

Expression of PCLP1 and Msln in Hepatic MCs During Liver Development

Msln is known to be a general marker for MCs. IHC showed that a single cell layer of mesothelial lining was specifically stained by both anti-Msln and anti-PCLP1 Abs in E16.5 liver sections (Figure 2*A*). In contrast to the lack of PCLP1 expression in adult MCs (Figure 1*A*), Msln was strongly expressed on adult MCs (Figure 2*A*) but not on fetal livers at earlier stages (data not shown). Cells highly expressing Msln were exclusively detected by flow cytometry in the surgically separated mesothelial tissue in PD0 and adult livers (Supplementary Figure 1*C*). These results suggested that MCs changed surface phenotypes from PCLP1^{+} to Msln^{+} during development. Consistent with the results of IHC, flow cytometry clearly showed that most of the PCLP1^{high} cells were Msln^{-} in E10.5 liver cell suspensions (Figure 2*B*). Interestingly, the fraction of Msln^{+} cells in the PCLP1^{high} cell population increased as fetal development progressed, while PCLP1^{+} cells in the Msln^{+} population decreased gradually after birth (Figure 2*B*). These results indicated that the expression of PCLP1 and Msln is developmentally regulated, and 3 developmental stages of MCs can be distinguished based on the expression of these 2 markers, that is, PCLP1^{high}Msln^{-}, PCLP1^{+}Msln^{+}, and PCLP1^{-}Msln^{+} MCs are the immature, intermediate, and mature stages of MCs, respectively.

Development of an In Vitro Culture System for Fetal MCs

To further characterize fetal MCs, we have developed an in vitro culture system for fetal MCs isolated by a cell sorter based on the expression of PCLP1 and/or Msln. The proliferation potential of MCs was determined by in vitro colony formation assay (see Supplementary Materials and Methods). Total numbers of colonies formed from 1×10^3 MCs isolated from E12.5, E18.5, and PD7 livers were 251.0 ± 5.7, 229.7 ± 19.7, and 95.3 ± 7.1, respectively, indicating that fetal hepatic MCs possessed higher proliferation potential than postnatal MCs. Adult hepatic MCs formed very few colonies (~3/1000 MCs; Figure 3*A* and *B*). Only PCLP1^{+}Msln^{+} MCs formed large colonies consisting of more than 300 cells, whereas the size of colonies formed from PD7 MCs was small (Figure 3*A* and *B*), indicating that hepatic MCs at the intermediate stage proliferate most actively and the proliferation potential of hepatic MCs declines after birth.

Interestingly, the cultivation of E12.5 PCLP1^{high}Msln^{-} cells changed the expression of PCLP1 and Msln, similar to the developmental change in vivo as shown in Figure 2*B* (Figure 3*C*). In this culture condition without exogenous cytokines, fetal MCs proliferated modestly but their proliferation ceased within several days. Additionally, they became PCLP1^{-}Msln^{+} MCs, a phenotype similar to adult MCs (Figure 3*C* and *D*). We found that addition of OSM and bFGF to culture medium synergistically promoted the expansion of fetal MCs (Figure 3*D*). Furthermore, 49% of the E12.5 PCLP1^{high} MCs maintained expression of PCLP1 after 6 days of cultivation in the presence of OSM and bFGF, while only 8% of the cells did so in their absence (Figure 3*E*). The continuous presence of OSM and bFGF in the culture medium maintained the expression of PCLP1 after the first passage, while their removal resulted in rapid down-regulation of PCLP1 expression and up-regulation of Msln expression (Figure 3*F* and Supplementary Figure 2). These results strongly suggested that OSM and bFGF could maintain immature characteristics of fetal MCs, whereas MCs proceeded to differentiate without them.

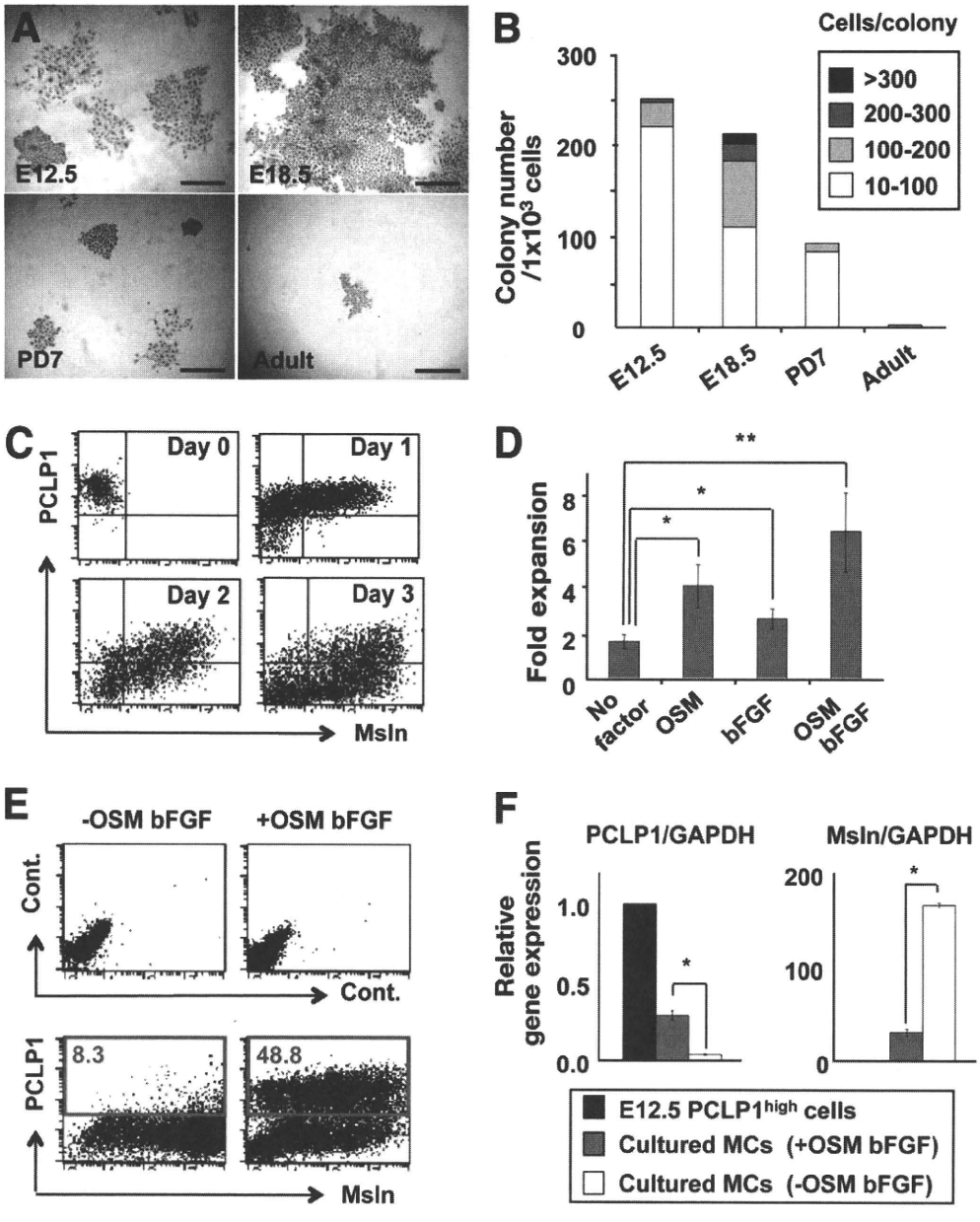

Figure 3. Expansion and differentiation of fetal MCs in vitro. (*A*) Colony-forming activity of hepatic MCs isolated from various stages of developing liver. Morphology of colonies formed from immature (E12.5), intermediate (E18.5), or mature (PD7 and Adult) MCs are shown. Colonies were stained with Giemsa solution after 6 days in culture. *Scale bars* = 80 μm. (*B*) Quantification of colony-forming potentials of MCs isolated from E12.5, E18.5, PD7, or adult liver. Averages of 3 wells for each sample are indicated. (*C*) Flow cytometry of cultured PCLP1^{high}Msln^{-} cells. Sorted cells from E12.5 liver were incubated and stained with anti-PCLP1 and anti-Msln Abs at the indicated time points. (*D*) Proliferation of fetal MCs in vitro. Flk1^{-}PCLP1^{high} cells sorted from E12.5 livers were cultured in the presence or absence of cytokines (10 ng/mL each) as indicated, and cell numbers were determined at day 6. Averages of 3 wells for each sample are shown. *$P < .05$, **$P < .01$; Student *t* test. (*E*) Flow cytometry of cultured MCs with anti-PCLP1 and anti-Msln Abs. Freshly isolated E12.5 Flk1^{-}PCLP1^{high} cells were cultured for 6 days in the presence or absence of OSM and bFGF and analyzed by flow cytometry. *Red lines* and *numbers* in the *lower panels* indicate PCLP1^{+} cell populations and their percentages, respectively. (*F*) Quantitative RT-PCR analysis for expression of PCLP1 and Msln in freshly isolated E12.5 PCLP1^{high} cells and cultured MCs. The actual ratios of marker/GAPDH in PLCP1^{high} cells and cultured cells (+OSM bFGF or −OSM bFGF) are as follows: PCLP1, 2.1×10^{-1}, 8.0×10^{-2}, and 7.5×10^{-3}; Msln, 1.8×10^{-3}, 6.6×10^{-2}, and 3.0×10^{-1}. *$P < .00003$; Student *t* test.

Fetal Hepatic MCs Are a Rich Source of Growth Factors for Hepatoblasts

It is known that MCs possess characteristics of both epithelial and mesenchymal cells,[7] but precise information about gene expression and other developmental characteristics of MCs remains limited. Therefore, microarray analysis was performed to compare gene expression profiles of E12.5 PCLP1^{high}Msln^{-} MC progenitors with adult Msln^{+} MCs (National Center for Biotechnology Information Gene Expression Omnibus accession no. GSE 18937). We found that MCs changed their gene expression profile drastically dur-

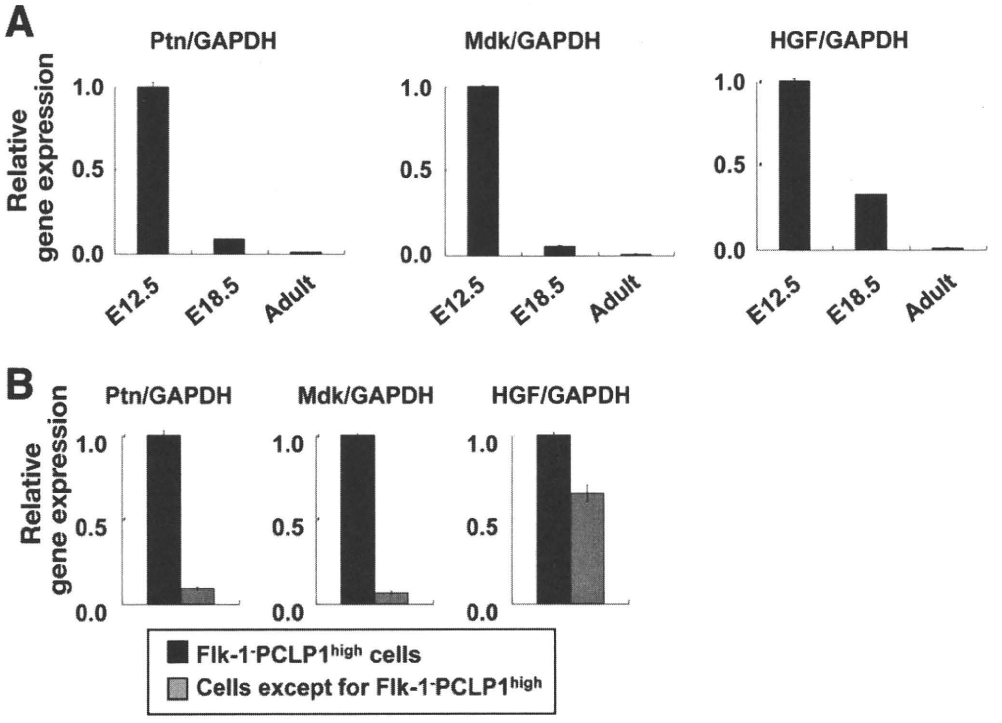

Figure 4. Expression of growth factors in liver cells. (*A*) Quantitative RT-PCR analysis for growth factors in MCs at distinct developmental stages. E12.5 Flk1^{-}PCLP1^{high} cells, E18.5 Msln^{+} cells, and adult Msln^{+} cells were isolated by a cell sorter and used for analyses. The actual ratios of factor/GAPDH in E12.5, E18.5, and adult MCs are as follows: Ptn, 3.9×10^{-1}, 4.0×10^{-2}, and 2.9×10^{-3}; Mdk, 1.0×10^{-1}, 6.1×10^{-3}, and 5.1×10^{-4}; HGF, 2.6×10^{-3}, 1.1×10^{-3}, and 4.7×10^{-4}. (*B*) Quantitative RT-PCR analysis of growth factors in Flk1^{-}PCLP1^{high} cells and the other cells at E12.5. The actual ratios of growth factor/GAPDH in Flk1^{-}PCLP1^{high} cells and the other cells are as follows: Ptn, 3.9×10^{-1} and 4.1×10^{-2}; Mdk, 1.0×10^{-1} and 7.8×10^{-3}; HGF, 2.6×10^{-3} and 1.6×10^{-3}.

ing development and that various signaling molecules were expressed in both fetal and adult MCs. In the list of soluble mediators whose expression in E12.5 MCs was more than 5-fold higher than in adult MCs (Supplementary Table 1), there were several growth factors known to promote proliferation of hepatocytes. Ptn is known to be a mitogen for adult hepatocytes[4,5] and was shown to be expressed highly in the STM and the hepatic MC layer of rat embryos.[5] Mdk is a molecule structurally related to Ptn.[4] Consistent with the microarray analysis, quantitative reverse-transcription (RT)-PCR analysis revealed that Ptn and Mdk were highly expressed in E12.5 MCs and became gradually down-regulated during ontogeny (Figure 4*A*). HGF was also expressed in E12.5 MCs, although its expression level was much lower than those of Ptn and Mdk (see the legend for Figure 4*A*). Furthermore, these growth factors were expressed more abundantly in MCs at E12.5 compared with non-MCs that contained hepatocytes, ECs, mesenchymal cells, and blood cells (Figure 4*B*). The expression of insulin-like growth factor 2 was detected at high levels in fetal MCs, although it was also expressed in fetal hepatocytes (data not shown). Importantly, all of these factors were remarkably down-regulated during development and were hardly detectable in adult MCs (Figure 4*A*). These observations suggested the intriguing possibility that fetal hepatic MCs play an active role in the proliferation and/or differentiation of hepatic cells in the developing liver.

Fetal MCs Promote Expansion of Hepatoblasts in a Paracrine Manner by Secreting Soluble Factors

To examine whether fetal MCs contribute to proliferation of hepatoblasts, we designed a coculture system of fetal hepatocytes with fetal MCs. Because the number of MCs isolated from fetal livers was too small for such experiments, we took advantage of fetal MCs expanded in vitro. Fetal hepatoblasts were isolated from E14.5 livers with anti-Dlk1 Ab as reported previously[18] and cultured with or without fetal MCs expanded in vitro using a 3-μm pored Transwell (Figure 5*A*). Hepatoblasts proliferated actively in the presence of Ptn or Mdk (Figure 5*B*) and in the coculture with MCs (Figure 5*C* and *D*), which was confirmed by WST-1 assay. MCs isolated from a later stage (E18.5) also enhanced the proliferation of fetal hepatocytes, and E16.5 hepatocytes also proliferated by coculture with later-stage MCs (Supplementary Figure 3 and data not shown). Importantly, MCs cultured without OSM and bFGF before coculture failed to stimulate the proliferation of hepatoblasts (Figure 5*C*). These MCs also exhibited a cell surface phenotype similar to differentiated MCs (Figure 3*E* and *F*), and growth factor expression was remarkably reduced, similar to adult MCs (Figures 5*E* and 4*A*). By contrast, MCs cultured in the presence of OSM and bFGF expressed growth factors at levels comparable to E18.5 MCs (Figures 5*E* and 4*A*). These results indicated that fetal hepatic MCs possess the potential to promote the proliferation of hepatocytes by secreting soluble factors, and the 2 types of MCs used for coculture exhibit the characteristics of fetal undifferentiated MCs and adult MCs in vivo, respectively.

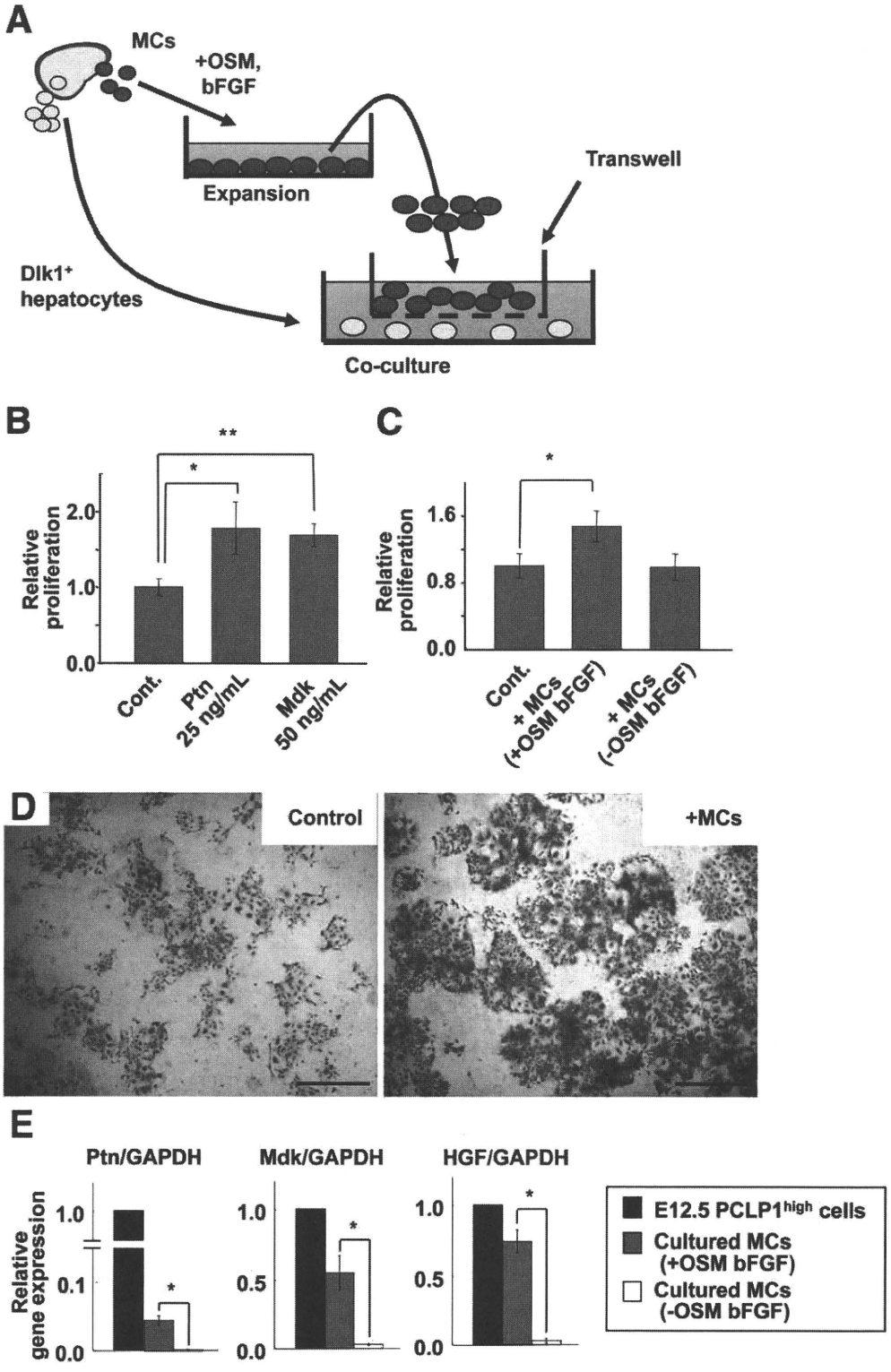

Figure 5. Hepatic MCs promote the proliferation of hepatoblasts in the coculture system. (*A*) The coculture system of fetal hepatoblasts and hepatic MCs separated by Transwell. After culturing of freshly isolated MCs in the presence of OSM and bFGF, the expanded MCs were used for coculture with Dlk1$^+$ hepatoblasts. (*B*) Proliferation of hepatoblasts in coculture system. Dlk1$^+$ cells sorted from E14.5 livers were cultured in the presence of growth factors as indicated. Growth of hepatocytes was measured by WST-1 assay after 4 days of culture. The averages for 3 wells of each sample are shown. $^*P < .03$; $^{**}P < .004$; Student *t* test. (*C*) Proliferation of E14.5 Dlk1$^+$ cells cultured with in vitro expanded E12.5 MCs. After primary expansion of MCs, the cells were cultured for an additional 5 days in the presence or absence of OSM and bFGF before coculture. Growth of hepatocytes was measured by WST-1 assay as in *B*. $^*P < .007$; Student *t* test. (*D*) Appearance of hepatocytes stained with Giemsa solution after 3 days of coculture. (*E*) Quantitative RT-PCR analysis of growth factors in freshly isolated E12.5 PCLP1^{high} cells and cultured MCs. The actual ratios of marker/GAPDH in PLCP1^{high} cells and cultured cells with OSM and bFGF (+OSM bFGF) or without them (−OSM bFGF) before coculture are as follows: Ptn, 1.4, 5.7 × 10^{-2}, and 2.6 × 10^{-3}; Mdk, 1.8 × 10^{-2}, 1.0 × 10^{-2}, and 5.5 × 10^{-4}; HGF, 4.1 × 10^{-4}, 3.0 × 10^{-4}, and 1.1 × 10^{-5}. $^*P <$ .0005; Student *t* test.

In Vivo Function of Fetal Hepatic MCs

Wilms' tumor 1 homologue (WT1) is a Zn finger protein that is known to play a critical role in organogenesis of multiple organs, including the kidney, heart, diaphragm, spleen, gonad, and liver. WT1 is also known as a marker for the mesothelial lineage,[7] and it is believed to be a regulator of mesothelial development. In mouse fetal liver, WT1 was reported to be expressed strongly in coelomic epithelial cells,[21] which correspond to hepatic MCs. In fact, WT1 was mainly expressed in MCs, whereas its expression was hardly detectable in non-MCs, including hepatocytes, ECs, mesenchymal cells, and blood cells

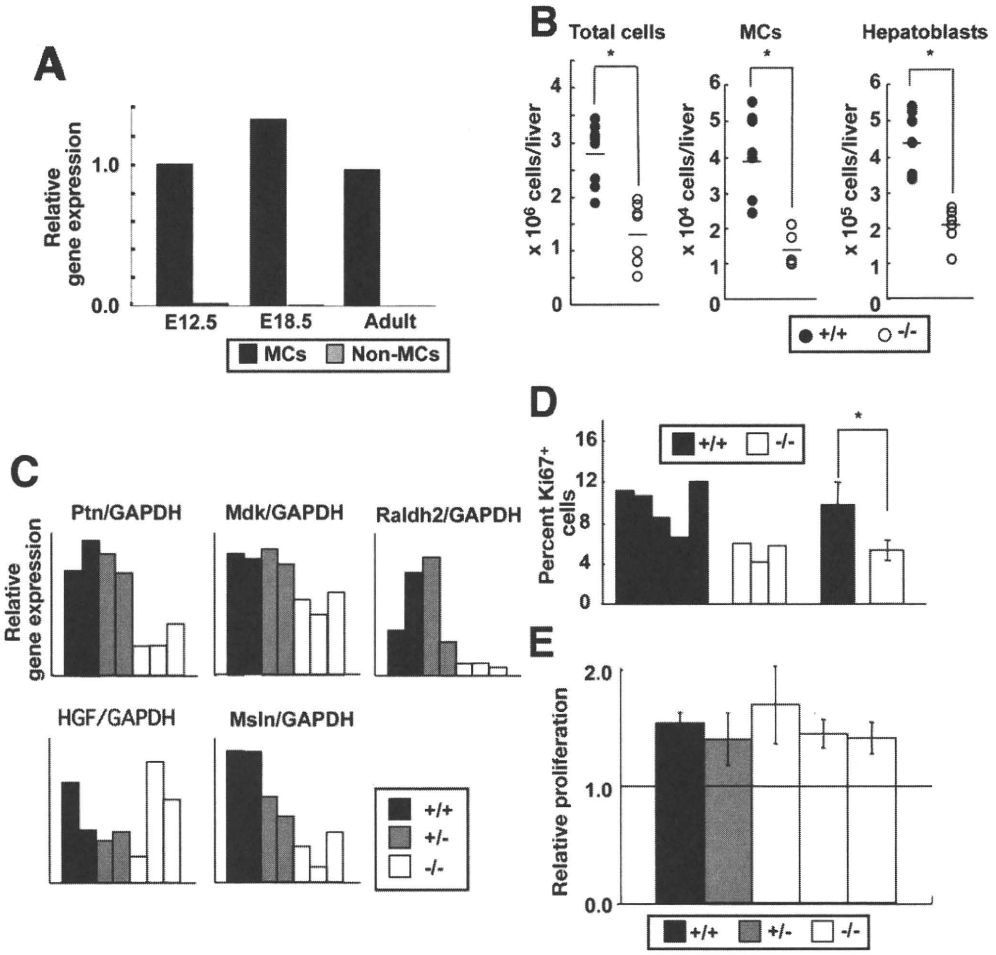

Figure 6. Characteristics of hepatic MCs in WT1-deficient embryos. (*A*) Quantitative RT-PCR analysis of WT1 expression in MCs or non-MCs. The relative gene expression of WT1/GAPDH in MCs and non-MCs at distinct developmental stages is shown. The actual ratios of WT1/GAPDH in MCs and non-MCs for E12.5, E18.5, and adults are 2.4×10^{-4} and 3.2×10^{-6}, 3.7×10^{-4} and 3.5×10^{-7}, and 2.3×10^{-4} and 2.8×10^{-6}, respectively. (*B*) The numbers of total fetal liver cells (*left panel*; +/+, n = 8; −/−, n = 8), PCLP1^{high} cells (*middle panel*; +/+, n = 7; −/−, n = 6), and Dlk1^{+} cells (right panel, +/+, n = 7; −/−, n = 6) per liver of E13.5 embryos are shown. *$P < .0007$; Student *t* test. (*C*) Quantitative RT-PCR analysis in PCLP1^{high} MCs of E13.5 littermates. Relative gene expression is shown. *Filled*, *gray*, and *open bars* indicate an individual embryo with +/+, +/−, and −/− genotype, respectively. (*D*) The ratio of Ki67^{+} cells in PCLP1^{high} MCs between E13.5 WT1$^{+/+}$ and WT1$^{-/-}$ livers of littermates. The *right bars* show the difference between the 2 genotypes. *$P < .02$; Student *t* test. (*E*) Proliferation potential of Dlk1^{+} hepatoblasts derived from E13.5 WT1$^{+/+}$, WT1$^{+/-}$, and WT1$^{-/-}$ livers. Dlk1^{+} hepatoblasts of littermates with each genotype were sorted by a cell sorter and cocultured with or without in vitro expanded E12.5 WT1$^{+/+}$ MCs. Growth of hepatocytes was measured by WST-1 assay in triplicate cultures after 4 days of coculture. The ratios of the WST-1 value in culture with MCs to that without MCs are shown for each genotype. Note that there is no significant difference among genotypes. The experiment was repeated twice with similar results.

in the developing liver (Figure 6*A*). Consistent with a previous report,[21] WT1$^{-/-}$ embryos had smaller livers with incomplete lobulation compared with littermates with WT1$^{+/+}$ or WT1$^{+/-}$ genotypes at E13.5 (Supplementary Figure 4*A* and data not shown). The percentages of Flk1^{-}PCLP1^{high} MC progenitors in WT1$^{-/-}$ fetal livers were not reduced significantly compared with their littermates by flow cytometry (Supplementary Figure 4*B* and data not shown). However, the numbers of Flk1^{-}PCLP1^{high} MCs, Dlk1^{+} hepatoblasts, and total fetal liver cells were all reduced in WT1$^{-/-}$ animals (Figure 6*B*). Next, we isolated MCs to examine the expression of growth factors by quantitative RT-PCR. Ptn and Mdk were reduced in WT1$^{-/-}$ hepatic MCs compared with the littermates with WT1$^{+/+}$ or WT1$^{+/-}$ genotypes (Figure 6*C*). The expression of Msln in WT1$^{-/-}$ MCs was also severely reduced at E13.5, indicating that MC differentiation may also be impaired in WT1-deficient livers. In addition, the expression of retinaldehyde dehydrogenase 2 (RALDH2) was significantly reduced in WT1$^{-/-}$ MCs, consistent with the notion that retinoic acid regulates proliferation of MCs in vivo.[21] Proliferation of MCs might also be altered in these embryos. The percentages of Ki67^{+} cells in PCLP1^{high} MCs isolated from WT1$^{-/-}$ embryos were significantly reduced compared with those of WT1$^{+/+}$ embryos (Figure 6*D*). Coculture of Dlk1^{+}

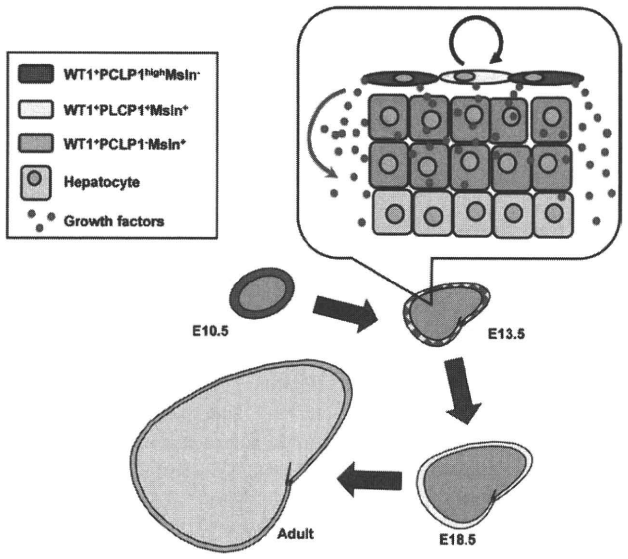

Figure 7. A model for hepatic MC development and its role in liver organogenesis. At an early stage of liver development, PCLP1^{high}Msln^{-} immature MCs cover the hepatic lobes (E10.5–12.5, *red*). The expression of Msln is up-regulated in MCs during fetal liver development, and most of the MCs become PCLP1^{+}Msln^{+} around birth (E18.5, *light yellow*). MCs provide hepatoblasts with multiple growth factors and they also proliferate actively during fetal stages, contributing to liver organogenesis. After birth, MCs become PCLP1^{-}Msln^{+} (*light green*), and their proliferation potential declines. MCs then switch their function from a niche for hepatoblasts to nonadhesive protective surfaces.

hepatocytes from WT1$^{-/-}$ or WT1$^{+/+}$ livers with WT1$^{+/+}$ MCs showed no significant difference in proliferation of hepatocytes among the different genotypes, indicating that the reduced proliferation of hepatocytes in WT1$^{-/-}$ fetal livers was not due to defects in hepatocytes (Figure 6*E*). From these results, we concluded that WT1-null hepatic MCs are defective in proliferation and the production of growth factors. These results strongly suggested that impaired development of hepatic MCs results in decreased proliferation of hepatocytes as well as abnormal morphogenesis of the liver.

Discussion

In this study, we show that splanchnic MCs are not only an inert protective sheet for coelomic organs but also change their characteristics dynamically during organogenesis. In the liver, at least 3 distinct developmental stages of MCs are recognized based on the expression of PCLP1 and Msln (Figure 7). PCLP1^{high}Msln^{-} immature MC progenitors at E10.5 define the border of each hepatic lobe. Furthermore, the proliferation and gene expression profile of hepatic MCs change dramatically during development. In particular, fetal hepatic MCs were shown to express various soluble factors, including hepatocyte mitogens such as Ptn, Mdk, and HGF, indicating that MCs function as a rich source of growth factors for hepatic cells in liver development (Figures 4 and 7). In fact, coculture experiments using MCs and Dlk1^{+} fetal hepatocytes clearly show that MCs provide growth factors for hepatocytes. Considering that mesenchymal cells derived from STM contribute to the commitment of foregut endodermal cells into the hepatic lineage and to the outgrowth of hepatoblasts at the onset of liver development, it is not surprising that the lateral plate mesoderm-derived mesothelial tissue plays an active role in liver development as a producer of growth factors. Consistent with the previous report by Suksaweang et al,[6] we observed that Ki67^{+}HNF4α^{+} proliferating hepatocytes were present more frequently in the peripheral region than in the central region of the lobes in developing mouse liver (Supplementary Figure 5 and Supplementary Table 2). These observations suggest that MCs contribute to liver growth and morphogenesis by providing mitotic stimuli and/or microenvironment for hepatocytes.

This idea is strongly supported by the analysis of WT1-deficient mice. Ijpenberg et al recently reported that the livers of WT1 mutant embryos are small, showing defects in the proliferation of coelomic epithelial cells and hepatocytes, lobulation, and differentiation of stellate cells during liver development.[21] Coelomic epithelial cells lining the liver of WT1-null embryos showed the reduction of Raldh2 expression, suggesting possible involvement of the retinoic acid signaling pathway in liver development as in the case of heart development that requires WT1-expressing epicardial cells and Raldh2.[22,23] However, it had been unclear why proliferation of hepatocytes was also impaired in WT1-deficient fetal livers. Isolation and characterization of PCLP1^{high} MCs from WT1$^{-/-}$ mice in this study show that proliferation of MCs and their production of growth factors, including Ptn and Mdk, are impaired in these embryos, whereas Dlk1^{+} cells from WT1$^{-/-}$ livers proliferate normally in response to WT1$^{+/+}$ MCs. The expression level of HGF was not affected in the absence of WT1, although the expression level of HGF in WT1$^{+/+}$ MCs was much lower than that of Ptn and Mdk. Thus, it is strongly suggested that the growth retardation of WT1-deficient livers is mainly due to the reduced proliferation of hepatic MCs and their insufficient production of mitogens for hepatocytes. Importantly, because MCs express various growth factors, there might be factors other than Ptn, Mdk, and HGF that also stimulate proliferation of hepatocytes.

Previous studies showed that WT1-expressing epicardial and serosal MCs are a source of coronary and gut vasculogenic cells, respectively.[8,10] It is thus of great interest to know whether immature PCLP1^{high}Msln^{-} cells also possess the potential to differentiate into nonmesothelial lineages. In fact, Pérez-Pomares et al reported that liver sinusoidal endothelial cells and mural cells in avian embryos were derived from the mesothelium.[11] We observed that some ALCAM^{+} cells were generated in the culture of E12.5 PCLP1^{high}ALCAM^{-} MCs (Supplemen-

tary Figure 6). Because ALCAM is specifically expressed in submesothelial cells that underlie the hepatic MC layer,[24] MCs may have a potential to give rise to those mesenchymal cells. Further studies on the differentiation potential of MCs may provide new insights in liver organogenesis.

Fetal liver is the major hematopoietic organ and contains numerous blood cells, which also contribute to hepatogenesis. We previously showed that OSM produced from blood cells stimulates the differentiation of fetal hepatoblasts in vitro.[25] After birth, hematopoiesis shifts to the bone marrow and OSM expression decreases in the liver. In this report, we show that OSM stimulates the proliferation of fetal hepatic MCs and maintains their immature characteristics, including the ability to support the proliferation of hepatoblasts. These results suggest the possible link between hematopoiesis and the proliferation of MCs and hepatoblasts in fetal liver and that OSM may play a role for the coordination of these cells.

In conclusion, this study reveals dynamic changes in characteristics of hepatic MCs during development and shows that hepatic MCs play an active role in organogenesis by providing growth factors for parenchymal cells. Besides liver development, fetal MCs may also be actively involved in the development of other organs.

Supplementary Material

Note: To access the supplementary material accompanying this article, visit the online version of *Gastroenterology* at www.gastrojournal.org, and at doi: 10.1053/j.gastro.2009.12.059.

References

1. Jung J, Zheng M, Goldfarb M, et al. Initiation of mammalian liver development from endoderm by fibroblast growth factors. Science 1999;284:1998–2003.
2. Rossi JM, Dunn NR, Hogan BL, et al. Distinct mesodermal signals, including BMPs from the septum transversum mesenchyme, are required in combination for hepatogenesis from the endoderm. Genes Dev 2001;15:1998–2009.
3. Matsumoto K, Yoshitomi H, Rossant J, et al. Liver organogenesis promoted by endothelial cells prior to vascular function. Science 2001;294:559–563.
4. Muramatsu T. Midkine and pleiotrophin: two related proteins involved in development, survival, inflammation and tumorigenesis. J Biochem 2002;132:359–371.
5. Asahina K, Sato H, Yamasaki C, et al. Pleiotrophin/heparin-binding growth-associated molecule as a mitogen of rat hepatocytes and its role in regeneration and development of liver. Am J Pathol 2002;160:2191–2205.
6. Suksaweang S, Lin CM, Jiang TX, et al. Morphogenesis of chicken liver: identification of localized growth zones and the role of beta-catenin/Wnt in size regulation. Dev Biol 2004;266:109–122.
7. Herrick SE, Mutsaers SE. Mesothelial progenitor cells and their potential in tissue engineering. Int J Biochem Cell Biol 2004;36:621–642.
8. Perez-Pomares JM, Carmona R, Gonzalez-Iriarte M, et al. Origin of coronary endothelial cells from epicardial mesothelium in avian embryos. Int J Dev Biol 2002;46:1005–1013.
9. Que J, Wilm B, Hasegawa H, et al. Mesothelium contributes to vascular smooth muscle and mesenchyme during lung development. Proc Natl Acad Sci U S A 2008;105:16626–16630.
10. Wilm B, Ipenberg A, Hastie ND, et al. The serosal mesothelium is a major source of smooth muscle cells of the gut vasculature. Development 2005;132:5317–5328.
11. Pérez-Pomares JM, Carmona R, Gonzalez-Iriarte M, et al. Contribution of mesothelium-derived cells to liver sinusoids in avian embryos. Dev Dyn 2004;229:465–474.
12. Kerjaschki D, Sharkey DJ, Farquhar MG. Identification and characterization of podocalyxin—the major sialoprotein of the renal glomerular epithelial cell. J Cell Biol 1984;98:1591–1596.
13. Horvat R, Hovorka A, Dekan G, et al. Endothelial cell membranes contain podocalyxin—the major sialoprotein of visceral glomerular epithelial cells. J Cell Biol 1986;102:484–491.
14. Hara T, Nakano Y, Tanaka M, et al. Identification of podocalyxin-like protein 1 as a novel cell surface marker for hemangioblasts in the murine aorta-gonad-mesonephros region. Immunity 1999;11:567–578.
15. Doyonnas R, Nielsen JS, Chelliah S, et al. Podocalyxin is a CD34-related marker of murine hematopoietic stem cells and embryonic erythroid cells. Blood 2005;105:4170–4178.
16. Rump A, Morikawa Y, Tanaka M, et al. Binding of ovarian cancer antigen CA125/MUC16 to mesothelin mediates cell adhesion. J Biol Chem 2004;279:9190–9198.
17. Kreidberg JA, Sariola H, Loring JM, et al. WT-1 is required for early kidney development. Cell 1993;74:679–691.
18. Tanimizu N, Nishikawa M, Saito H, et al. Isolation of hepatoblasts based on the expression of Dlk/Pref-1. J Cell Sci 2003;116:1775–1786.
19. Tanaka M, Okabe M, Suzuki K, et al. Mouse hepatoblasts at distinct developmental stages are characterized by expression of EpCAM and DLK1: drastic change of EpCAM expression during liver development. Mech Dev 2009;126:665–676.
20. Suzuki K, Tanaka M, Watanabe N, et al. p75 Neurotrophin receptor is a marker for precursors of stellate cells and portal fibroblasts in mouse fetal liver. Gastroenterology 2008;135:270–281, e3.
21. Ijpenberg A, Perez-Pomares JM, Guadix JA, et al. Wt1 and retinoic acid signaling are essential for stellate cell development and liver morphogenesis. Dev Biol 2007;312:157–170.
22. Niederreither K, Subbarayan V, Dolle P, et al. Embryonic retinoic acid synthesis is essential for early mouse post-implantation development. Nat Genet 1999;21:444–448.
23. Perez-Pomares JM, Phelps A, Sedmerova M, et al. Experimental studies on the spatiotemporal expression of WT1 and RALDH2 in the embryonic avian heart: a model for the regulation of myocardial and valvuloseptal development by epicardially derived cells (EPDCs). Dev Biol 2002;247:307–326.
24. Asahina K, Tsai SY, Li P, et al. Mesenchymal origin of hepatic stellate cells, submesothelial cells, and perivascular mesenchymal cells during mouse liver development. Hepatology 2009;49:998–1011.
25. Kinoshita T, Sekiguchi T, Xu MJ, et al. Hepatic differentiation induced by oncostatin M attenuates fetal liver hematopoiesis. Proc Natl Acad Sci U S A 1999;96:7265–7270.

Received June 30, 2009. Accepted December 31, 2009.

Reprint requests

Address requests for reprints to: Atsushi Miyajima, PhD, Laboratory of Cell Growth and Differentiation, Institute of Molecular

and Cellular Biosciences, University of Tokyo, 1-1-1 Yayoi, Bunkyo-ku, Tokyo 113-0032, Japan. e-mail: miyajima@iam.u-tokyo.ac.jp; fax: (81) 3-5841-8475.

Acknowledgments

The authors thank Dr R. Nishinakamura and Dr S. Kawamata for providing us with $WT1^{+/-}$ mice and anti-ALCAM antibody, respectively, and Drs J. James, T. Itoh, N. Tanimizu, and H. Nonaka for valuable discussions and critical reading of the manuscript.

Transcript profiling (expression microarray): National Center for Biotechnology Information Gene Expression Omnibus accession no. GSE 18937. (http://www.ncbi.nlm.nih.gov/geo/query/acc.cgi?acc=GSE18937).

Conflicts of interest

The authors disclose no conflicts.

Funding

Supported in part by a research grant from the Ministry of Health, Labor and Welfare and Grant-in-Aid for Scientific Research and Global COE Project of the Ministry of Education, Culture, Sports, Science and Technology of Japan.